

Deciphering the tumor microenvironment in pancreatic cancer

—

Infiltration of tumor-associated macrophages and their role in tumor progression

Kathrin Grabichler

Vollständiger Abdruck der von der TUM School of Medicine and Health der Technischen Universität München zur Erlangung einer

Doktorin der Medizin (Dr.med.)

genehmigten Dissertation.

Vorsitz: Prof. Dr. Gabriele Multhoff

Prüfende der Dissertation:

1. Prof. Dr. Dieter Saur
2. Prof. Dr. Marc Schmidt-Supprian

Die Dissertation wurde am 23.05.2024 bei der Technischen Universität München eingereicht und durch die TUM School of Medicine and Health am 04.02.2025 angenommen.

I. TABLE OF CONTENTS

I. TABLE OF CONTENTS.....	1
II. LIST OF FIGURES.....	4
III. ABBREVIATIONS.....	5
IV. ABSTRACT.....	6
V. ZUSAMMENFASSUNG.....	7
1. INTRODUCTION.....	8
1.1. Pancreatic ductal adenocarcinoma (PDAC).....	8
1.2. The tumor microenvironment of PDAC.....	8
1.2.1. <i>Impact of oncogenic KRAS on the TME</i>	8
1.2.2. <i>Distinct PDAC cell subtypes</i>	9
1.2.3. <i>Stromal and immune cell compartments in the TME</i>	9
1.3. Tumor-associated macrophages (TAMs).....	10
1.3.1. Subpopulations.....	10
1.3.1.1. <i>The M1-/ M2-phenotype</i>	10
1.3.1.2. <i>Macrophage origin</i>	11
1.3.2. Impact on tumor progression and therapy response.....	11
1.4. Mouse models of PDAC.....	12
1.5. Objectives of this work.....	13
2. MATERIALS.....	14
2.1. Mouse PDAC cell lines.....	14
2.2. Antibodies.....	14
2.2.1. <i>Multi-colour Confocal Microscopy</i>	14
2.2.2. <i>Multi-colour Flow cytometry</i>	15
2.3. Media and reagents.....	16
2.4. Kits.....	17
2.5. Software and databases.....	17
3. METHODS.....	18
3.1. Animal experiments.....	18

3.1.1. <i>Mouse strains</i>	18
3.1.2. <i>Mouse genotyping and dissection</i>	18
3.1.3. <i>Orthotopic implantation of PDAC cells in mice</i>	19
3.1.4. <i>Nintedanib and Trametinib treatment of tumor bearing mice</i>	19
3.2. <i>Histopathological analysis of PDAC cohort</i>	19
3.3. <i>Flow cytometry analysis of innate and adaptive immune cells</i>	19
3.4. <i>Immunofluorescence analysis of immune cells</i>	20
3.4.1. <i>Tissue fixation and tissue section</i>	20
3.4.2. <i>Antibody-based staining</i>	20
3.4.3. <i>TAM imaging with confocal microscope</i>	20
3.4.4. <i>TAM counting with ImageJ</i>	21
3.5. <i>Single cell RNA sequencing</i>	21
3.5.1. <i>Sample preparation</i>	21
3.5.2. <i>Library preparation and sequencing</i>	21
3.5.3. <i>Data pre-processing, integration and quality control</i>	21
3.5.4. <i>Dimensionality reduction and clustering</i>	22
3.5.5. <i>Gene Set Enrichment Analysis (GSEA)</i>	22
3.5.6. <i>Cell-type-specific analysis of macrophages</i>	22
4. RESULTS	23
4.1. Multimodal approach reveals inter- and intratumoral heterogeneity of the myeloid cell compartment in <i>Kras</i>^{G12D}-driven PDAC	24
4.2. Different molecular PDAC subtypes display considerable distinctions in their myeloid cell compartment	31
4.3. Combinatorial drug treatment leads to an increase of proinflammatory features of TAMs ..	40
4.4. Conclusion	45
5. DISCUSSION	46
5.1. Impacts on TAM phenotype in PDAC	46
5.1.1. <i>Genetic alterations</i>	46
5.1.2. <i>Transcriptional subtypes</i>	47
5.2. TAM characteristics	48
5.2.1. <i>Immunosuppressive pathways</i>	48

5.2.2. <i>Involvement in therapy response</i>	49
5.3. Outlook	50
6. References	50
7. PUBLICATION	60
8. ACKNOWLEDGEMENTS	61

II. LIST OF FIGURES

Figure 1. Overview of experimental workflow for a systematic analysis of the TME of endogenous <i>Kras</i> ^{G12D} -driven PDAC	24
Figure 2. Characterization of immune cell infiltration in <i>Kras</i> ^{G12D} -driven PDAC	25
Figure 3. Identification of macrophage subpopulations in endogenous <i>KRAS</i> ^{G12D} -driven PDAC by immunofluorescence	28
Figure 4. scRNA-seq reveals distinct subpopulations of TAMs in endogenous <i>Kras</i> ^{G12D} -driven PDAC	31
Figure 5. TME characterization in orthotopically implanted PDAC of classical and mesenchymal cell lines	33
Figure 6. Identification of macrophage subpopulations in transcriptional PDAC subtypes by immunofluorescent imaging	35
Figure 7. scRNA-seq analysis reveals distinct clusters of TIMs in classical and mesenchymal PDAC subtypes	37
Figure 8. Identification of macrophage subclusters in molecular PDAC subtypes displaying distinct characteristics	39
Figure 9. Characterization of TME in context of combinatorial drug treatment with Trametinib and Nintedanib of mice orthotopically implanted with <i>Kras</i> ^{G12D} -driven PDAC cell lines	41
Figure 10. Combinatorial treatment with Trametinib and Nintedanib enhances infiltration of M1-like macrophages into the tumor tissue	43
Figure 11. Summary of key immunosuppressive TAM -features found by scRNA-seq of distinct molecular PDAC subtypes	45

III. ABBREVIATIONS

Ag	Antigen
BMD	Bone marrow derived
CAF	Cancer-associated fibroblasts
CyTOF	Cytometry by time of flight
DC	Dendritic cells
DMEM	Dulbecco's modified eagle medium
ECM	Extracellular matrix
EGF	Epidermal growth factor
FCS	Fetal calve serum
FFPE	Formalin fixed paraffin embedded
GEM	Gel-bead in emulsion
GEMM	Genetically engineered mouse models
H&E	Hematoxylin and eosin
HSC	Hematopoietic stem cell
ICB	Immune checkpoint blockade
loxP	Locus of X-over P1
LPS	Lipopolysaccharide
LSL	LoxP-stop-LoxP
MDSC	Myeloid derived suppressor cells
MHC	Major histocompatibility complex
NO	Nitric oxide
PanIN	Pancreatic intraepithelial neoplasm
PBS	Phosphate buffered saline
PCR	Polymerase chain reaction
PDAC	Pancreatic ductal adenocarcinoma
PD-L1	Programmed death-ligand 1
PSC	Pancreatic stellate cells
RNA	Ribonucleic acid
scRNA-seq	Single-cell RNA sequencing
TAM	Tumor-associated macrophages
Th-cell	T-helper cell
TIM	Tumor-infiltrating myeloid cells
TME	Tumor microenvironment
TR	Tissue-resident
Treg	Regulatory T-cells
UMAP	Uniform Manifold Approximation and Projection
UMI	Unique molecular identifier
VEGF	Vascular endothelial growth factor

IV. ABSTRACT

Pancreatic ductal adenocarcinoma (PDAC) is a manifold cancer-type, comprising a heterogenous genetic landscape. Its unique tumor microenvironment (TME) is known to harbor a variety of immunosuppressive cells, including an abundance of tumor-associated macrophages (TAMs). However, there is still a lack of a clear characterization concerning their subpopulations and key immunosuppressive features. Moreover, hitherto the impact of genetic alterations and distinct molecular subtypes on the polarization of immune cells and thereby on tumor progression and therapy response is unknown. Hence, we performed a systematic characterization of TAM subsets in a *Kras*^{G12D}-driven model and in the two major molecular subtypes (classical and mesenchymal) of PDAC.

In this study, we analyze the monocytes and macrophages in the TME of two genetically well-defined PDAC cohorts, emerging of tumor samples of an endogenous or an orthotopic implanted mouse model. Therefore, we used a multimodal approach including immunofluorescent imaging, flow cytometry and single cell RNA-sequencing (scRNA-seq) analysis. Our results showed, *Kras*^{G12D}-driven PDAC displays great inter- and intratumoral heterogeneity of the TME, majorly concerning myeloid cells. Additionally, our findings elucidated notable differences of the TME composition, especially regarding the number and phenotype of TAM subpopulations, between the two major transcriptional subtypes of PDAC. Of these, the mesenchymal one being predominantly infiltrated with macrophages. The scRNA-seq analysis of our distinct PDAC cohorts revealed two key immunosuppressive markers of TAMs. Thereof, the complement factors were exhibited by tissue-resident macrophages of both molecular subtypes. For *Spp1* instead, being strikingly associated with hypoxic signatures, we found a greater leverage of the mesenchymal subtype.

In this work, we performed a systematic characterization of TAM subpopulations in PDAC. Our results uncover their major immunosuppressive pathways, including their differences in distinct molecular subtypes, and highlights them as potential therapeutic vulnerabilities. Therewith, these findings could help to improve future immunotherapeutic approaches of pancreatic cancer.

V. ZUSAMMENFASSUNG

Das duktales Adenokarzinom des Pankreas (PDAC) ist eine komplexe Krebserkrankung, die mit einer heterogenen genetischen Landschaft einhergeht. Ihr einzigartiges Tumormikromilieu beherbergt eine Vielzahl immunosuppressiver Zellen, einschließlich einer Fülle von tumor-assoziierten Makrophagen (TAMs). Bis heute fehlt eine eindeutige Charakterisierung ihrer Subpopulationen, sowie ihrer wichtigsten immunosuppressiven Marker. Unbekannt ist bisher darüber hinaus der Einfluss von genetischen Veränderungen und verschiedenen molekularen Subtypen auf die Polarisierung von Immunzellen. Damit auch ihr Einwirken auf Tumorwachstum und Therapieansprechen. Daher wurde in der vorliegenden Arbeit eine systematische Analyse von Untergruppen der TAMs in einem *Kras*^{G12D}-gesteuertem Mausmodell als auch in den beiden wichtigsten molekularen Subtypen (klassisch und mesenchymal) von PDAC durchgeführt.

In dieser Studie wurden Monozyten und Makrophagen aus dem Tumormikromilieu von zwei genetisch eindeutig definierten PDAC-Kohorten analysiert. Die Tumorstoffen hierfür stammten aus unserem endogenen oder unserem orthotop implantierten Mausmodell. Der von uns verwendete multimodale Ansatz umfasste die Durchführung von Immunofluoreszenz-Bildgebung, Durchflusszytometrie und Einzelzell-RNA Sequenzierung. Unsere Ergebnisse zeigten eine große inter- als auch intratumorale Heterogenität des Tumormikromilieus in unserer *Kras*^{G12D}-gesteuerten PDAC-Kohorte, besonders in Bezug auf myeloische Zellen. Darüber hinaus offenbarten unsere Resultate bemerkenswerte Unterschiede zwischen den beiden wichtigsten molekularen Subtypen von PDAC bezüglich deren Zusammensetzung des Tumormikromilieus. Die Abweichungen betrafen vor allem die Anzahl und den Phänotyp von TAM-Subpopulationen, so zeigte der mesenchymale im Vergleich zum klassischen Subtyp eine eindeutige Prädominanz von Makrophagen. Die Einzelzell-RNA Sequenzierung unserer verschiedenen PDAC-Kohorten rückte besonders zwei immunosuppressive Marker von TAMs in den Vordergrund. Die Komplementfaktoren, welche von geweberesidenten Makrophagen beider molekularer Subtypen exprimiert wurden. Zudem *Spp1*, welches eine starke Assoziation zu hypoxischen Merkmalen zeigte und vor allem vom mesenchymalen Subtyp exprimiert wurde.

Diese Arbeit beschreibt die Durchführung einer systematischen Charakterisierung von TAM-Subpopulationen in PDAC. Unsere Ergebnisse heben die Schlüsselemente ihrer immunosuppressiven Pfade, einschließlich der Unterschiede zwischen den molekularen Subtypen, hervor. Darüber hinaus unterstreichen sie diese als potenzielle therapeutische Angriffspunkte.

Zusammengenommen könnten unsere Erkenntnisse dazu beitragen, die Wirksamkeit zukünftiger Immuntherapien des Pankreaskarzinoms zu verbessern.

1. INTRODUCTION

1.1. Pancreatic ductal adenocarcinoma (PDAC)

Worldwide neoplastic diseases are an enduring major issue in health care. By now, behind cardiovascular diseases cancer is the second leading cause of death in the US (Siegel, Miller, Wagle, & Jemal, 2023). Whereas over the past decades for most other cancer types the mortality rate is decreasing, it stays almost stable for pancreatic cancer. The absolute number of patients dying because of pancreatic cancer even goes up. (Carioli et al., 2021; Grossberg et al., 2020). Despite great efforts of improving the survival rate already done it is proclaimed that pancreatic cancer will even rise to the second leading cause of cancer related death before 2030 (Rahib et al., 2014). The great malignancy of this disease is also reflected by the poor 5-year survival rate of 12% for patients diagnosed between 2012 and 2018 according to the statistics provided by the SEER (Surveillance, Epidemiology, and End Results Program) of the National Cancer Institute (Siegel et al., 2023). Pancreatic ductal adenocarcinoma (PDAC) accounts for over 90% of pancreatic cancer (Feldmann, Beaty, Hruban, & Maitra, 2007). There is a broad range of risk factors as high age, smoking and alcohol abuse contributing to the development of pancreatic cancer particularly in the affluent society (Bosetti et al., 2012; Raimondi, Lowenfels, Morselli-Labate, Maisonneuve, & Pezzilli, 2010; Wang, Gou, Jin, Xiao, & Fang, 2016). Reasons for the poor outcome of PDAC are a lack of revealing screening tools and missing of early and specific symptoms (Kim et al., 2004; L. Zhang, Sanagapalli, & Stoita, 2018). That is why pancreatic cancer is mostly diagnosed in advanced and already metastasized stages (Brennan, Kattan, Klimstra, & Conlon, 2004; S. R. Lee, Kim, Son, Yoo, & Shin, 2013). This results in 80 to 90% of PDAC cases being unresectable at time of diagnosis. Unfortunately, surgical resection remains the only potentially curative option hitherto (Ilic & Ilic, 2016; Khorana et al., 2017). To finally improve the long-term survival of PDAC patients it is crucial to eliminate risk factors, achieve early diagnosis and progress in therapy. As especially pancreatic cancer has a diverse tumor microenvironment (TME) with a unique stromal and immune compartment which maintain an intense crosstalk with tumor cells. Thus, the multifaceted TME is not only able to hinder tumor growth, but is highly immunosuppressive and thereby supports tumor progression in multiple ways (Falcomatà et al., 2023; Ho, Jaffee, & Zheng, 2020; Manrai, Tilak, Dawra, Srivastava, & Singh, 2021).

1.2. The tumor microenvironment of PDAC

1.2.1. Impact of oncogenic *KRAS* on the TME

According to the Cancer Genome Atlas Research Network, over 90% of PDAC are carrying oncogenic *KRAS*-mutations ("Integrated Genomic Characterization of Pancreatic Ductal Adenocarcinoma," 2017), contributing to PDAC initiation by its downstream *RAF-MEK-ERK* pathway (Collisson et al., 2012). Oncogenic *KRAS* interferes with regular GTPase activity which results in a constitutive active Ras-state (Gibbs, Sigal, Poe, & Scolnick, 1984; McGrath, Capon, Goeddel, & Levinson, 1984). This causes acceleration of tumor cell growth in many cancer types, including PDAC (Ambrogio et al., 2018). As written in Hou et al.: "Oncogenic *KRAS* regulates almost all the cancer hallmarks" (Hou & Wang, 2022). This includes particularly remodeling of the TME by a great crosstalk between tumor cells and cells of the stromal and immune compartments (Dey et al., 2020; Pylayeva-Gupta, Grabocka, & Bar-Sagi, 2011; Tape et al., 2016) as well as supporting tumor cells to overcome anticancer immunity

(Coelho et al., 2017). Exemplarily, it was demonstrated that the upregulation of *GM-CSF* in an oncogenic *KRAS*-dependent manner leads to recruitment of immunosuppressive myeloid cells in pancreatic neoplasia (Bayne et al., 2012; Pylayeva-Gupta, Lee, Hajdu, Miller, & Bar-Sagi, 2012). As efforts directly targeting oncogenic *KRAS* have been rather unsuccessful over the past decades getting further insight into the different components of the closely related TME with its stromal and immune compartments is worth focusing on (Hou & Wang, 2022).

1.2.2. Distinct PDAC cell subtypes

Transcriptomic analysis of bulk RNA-sequencing data acquired by several research groups showed that pancreatic tumor cells can be divided into distinct subclusters. 2011, Collisson et al. proclaimed 3 different intrinsic subtypes of PDAC named “classical”, “quasi-mesenchymal” and “exocrine-like” (Collisson et al., 2011). Further research done by Bailey et al. revealed 4 subtypes named “squamous”, “pancreatic progenitor”, “immunogenic” and “aberrantly differentiated” (Bailey et al., 2016). Whereas Moffitt et al. published the presence of a “classical” and a “basal-like” PDAC subtype (Moffitt et al., 2015). Taking together their results comparing the distinct signatures of the presented subtypes they can be subsumed into 2 groups showing great differences in their histopathological features and tumor progression: The classical PDAC being well-differentiated and associated with a better prognosis and the mesenchymal PDAC being poorly differentiated and associated with a worse prognosis compared to the classical one (Bailey et al., 2016; Bärthel, Falcomatà, Rad, Theis, & Saur, 2023; Collisson et al., 2011; Moffitt et al., 2015; S et al., 2020). According to the COMPASS trial there is moreover a difference in response to therapy with the classical PDAC showing a better response to first line chemotherapy while the mesenchymal PDAC comes along with high resistance to standard therapy (Aung et al., 2018). Beyond distinct molecular PDAC subtypes Moffitt et al. takes in account the existence of stromal subtypes to label independently, naming them “normal” and “activated”. The “activated” stromal subtype being affiliated with poorer prognosis compared to the “normal” subtype and being defined with a gene set associated with macrophages (Moffitt et al., 2015). Also, Puleo et al. requires regarding the stromal compartments detached from the distinct PDAC subtypes as well as the great interplay between these heterogeneous groups (Puleo et al., 2018).

1.2.3. Stromal and immune cell compartments in the TME

The stromal compartment is important for response to injury and tissue homeostasis. In cancer it is redirected to form a TME that is favorable for successful tumor growth (Foster, Jones, Ransom, Longaker, & Norton, 2018; Ho et al., 2020). Compared to other tumor entities pancreatic cancer has a peerless desmoplastic stroma coming along with high hypovascularity and a TME containing a great amount of fibroblasts, endothelial cells and immune cells (Erkan et al., 2012; Neesse et al., 2011; Whatcott et al., 2015). The dense stroma is even labeled as a “histopathological hallmark of PDAC” (Ho et al., 2020) and in some tumors makes up to 80% of the whole tumor mass (Erkan et al., 2012). The role of the TME is heterogeneous, it can suppress tumor progression by its antitumorigenic potential, but in contrast also foster PDAC growth (Elyada et al., 2019; Öhlund et al., 2017). In fact, multiple studies suggest a complex interplay between pancreatic cancer cells and cells of the stromal and immune compartments (Ansari, Carvajo, Bauden, & Andersson, 2017; Tang, Kesavan, Nakada, & Yan, 2004; Tape et al., 2016). The TME in PDAC contains a numerous proportion of immunosuppressive cells like pancreatic stellate cells (PSC), regulatory T-cells (Treg), myeloid-derived suppressor cells (MDSC) and tumor-associated macrophages (TAM)

(Cortesi et al., 2021; Gomez Perdiguero & Geissmann, 2014; Ren et al., 2018). Of these, especially myeloid cells highly infiltrate into the tumor site, among them, TAMs being one of the largest proportion (Zhu et al., 2017) displaying their great immunosuppressive potential inter alia by impairing a normal effector T-cell function (CD8⁺ T-cells) (Ren et al., 2018; Veglia, Sanseviero, & Gabrilovich, 2021). Thus, the TME of PDAC is labeled as immunologically “cold” (Binnewies et al., 2018). Synoptical, the TME with its variable immune cells create a considerable cellular complexity (Binnewies et al., 2018; Dominguez et al., 2020) and a singular milieu being highly metastatic and able to overcome anti-cancer immunity (Bergman, Pinedo, & Peters, 2002; Tao et al., 2021). Even having the potential to impair therapeutical strategies (Fan et al., 2020). Exemplarily, PDAC owns a very pronounced resistance to immune checkpoint blockade (ICB) and therapeutic strategies being applied solely are unlikely to be effective. That is why combinatorial strategies also targeting or even reprogramming the immunosuppressive TME are needed. The attempt to overcome myeloid cell derived immunosuppression, so enhancing an effective T-cell response, being a potential future approach (Bear, Vonderheide, & O'Hara, 2020; Thorsson et al., 2018).

1.3. Tumor-associated macrophages (TAMs)

In the year 1880, Mechnikov first described cells with phagocytic capacity, later named macrophages (Mechnikov, 1988). Growing knowledge showed that macrophages own numerous functions beside their phagocytic activity. They are a highly heterogeneous and remarkable versatile immune population decisively contributing to tissue homeostasis by their regulation of tissue regeneration, maintenance and development (Cox, Pokrovskii, Vicario, & Geissmann, 2021; Gordon, Plüddemann, & Martinez Estrada, 2014; Martinez & Gordon, 2014; Ren et al., 2018). Thus, macrophages serve as a kind of omnipresent guardian observing its surroundings for marks of infection or tissue disorders like a sign of tumor growth (Cox et al., 2021; Pollard, 2004). In most solid tumors, including the TME of PDAC, myeloid cells in particular macrophages are predominant. After infiltrating the tumor tissue, they are called tumor-associated macrophages (TAMs) (Deng, Patel, Chiang, & Hou, 2022; Tjomsland et al., 2011; F. Zhao et al., 2009).

1.3.1. Subpopulations

1.3.1.1. The M1-/ M2-phenotype

Taking note of the considerable impact of TAMs to the TME in various cancer types, great efforts were done to elucidate phenotypic subpopulations of this complex immune cell population. First, Martinez and Gordon described a dichotomous concept of on the one hand so-called classically activated macrophages driven by the exposure to LPS, IFN γ or TNF α homing pro-inflammatory properties as high Antigen (Ag) presenting capacity and being potent effector cells able to kill foreign microorganisms and tumor cells. On the other hand naming alternatively activated macrophages driven by the exposure to IL-4 and IL-13 being anti-inflammatory and thereby owning tumor-supporting properties (Martinez & Gordon, 2014). Later Mills et al. claim the Th1/2 paradigm (T-helper cells). According to which the immune response of macrophages depends on the T-cell population activating them and thereby deeply influence their immune reactions. Thus, being activated by Th1-cells macrophages produce high levels of NO adopting the so-called M1-phenotype (resembling the classically activated) whereas activation through Th2-cells leads to increased L-Arginine

metabolism and a M2-phenotype (resembling the alternatively activated) (Mills, Kincaid, Alt, Heilman, & Hill, 2000). Mantovani et al. further particularized this concept by declaring the M1/M2-clusters as two extremes of a polarization spectrum and additionally subdividing the M2-cluster into three subgroups naming them M2a, M2b and M2c (Mantovani et al., 2004). Over the past years, there is rising evidence that the polarization of macrophages *in vivo* is even more complex. Suggesting a continuum between M1- and M2-like properties and even possible combinations of them. Especially in tumor context the phenotype of TAMs is deeply influenced by a tremendous range of extrinsic and intrinsic stimuli emphasizing the need of further research in elucidating distinct macrophage subpopulations (C. Lee et al., 2019; Swietlik et al., 2023; Yang, Liu, & Liao, 2020).

1.3.1.2. Macrophage origin

In many tissue organs, including the pancreas, there is a coexistence of two macrophage populations differing in their origin. The tissue-resident (TR) macrophages are generated and seeded during embryonic development and persist through adulthood. Under homeostatic conditions TR macrophages can self-maintain with only negligible contribution of hematopoietic stem cells (HSC). Compared with that the bone marrow – derived (BMD) macrophages derive from circulating monocytes. In case of disturbed homeostasis, the recruitment of BMD macrophages is upregulated to replenish a proportion of TAMs in the affected tissue (Calderon et al., 2015; Deng et al., 2022; Gomez Perdiguero et al., 2015). Zhu et al. demonstrated that TAM ontogeny contributes to the development of different phenotypes and functionality in a murine model of PDAC. BMD macrophages showing a higher capability of Ag-presentation whereas TR macrophages being profibrotic and contribute to ECM remodeling. Moreover, TR macrophages expanded during PDAC progression and are suggested to own higher protumor characteristics (Zhu et al., 2017). Thus, when studying the polarization status of TAMs, also their origin must be considered.

1.3.2. Impact on tumor progression and therapy response

By entering the cytokine milieu of the local TME, highly influenced by tumor and other stromal cells, TAMs get educated to specialized immunosuppressive cells with a mostly M2-like phenotype uniting a great range of protumor functions. Thereby, at least in large parts losing their tumor rejecting properties (Pollard, 2004; Solinas, Germano, Mantovani, & Allavena, 2009). TAMs are reported to foster tumor progression by contributing to its invasiveness and even acceleration of metastasis by secreting an abundance of immunosuppressive cytokines, chemokines and growth factors as *TGF β* and *EGF*. Additionally, TAMs induce the expression of MMPs and proangiogenic factors as *VEGF α* (Cox et al., 2021; DeNardo et al., 2009; Gordon et al., 2014; Kitamura, Qian, & Pollard, 2015; Veglia et al., 2021). Facilitating the immune escape of neoplastic cells, multiple ways were described how TAMs impede effective T-cell response suppressing CD8+ cytotoxic and Th1-cell activity, but boost the recruitment and differentiation of immunosuppressive Th2-cells and regulatory T-cells (Treg) (Aslan et al., 2020; Daley, Mani, Mohan, Akkad, Ochi, et al., 2017; Daley, Mani, Mohan, Akkad, Pandian, et al., 2017; Rodriguez et al., 2004; Seifert et al., 2016). Moreover, M2 polarized macrophages were shown to promote epithelial to mesenchymal transition (EMT) in a preclinical model of cancer, thereby contributing to the formation of a dense stroma and driving resistance to chemotherapy by hindering drug delivery (Liu et al., 2013; Pollard, 2004; Yang et al., 2020), also being involved in inducing resistance to ablative radiotherapy (Kalbasi et al., 2017) and relapse after

chemotherapy (Hughes et al., 2015; Larionova et al., 2019). High density of TAMs was linked to poor outcome in mouse models of cancer and human pancreatic cancer patients (DeNardo et al., 2009; Ries et al., 2014; Thorsson et al., 2018; Yu et al., 2019). Besides that, TAMs contribute to sustain chronic inflammation going along with high levels of reactive oxygen and nitrogen, thus being highly mutagenic and supporting cancer initiation (Pollard, 2004). Being able to benefit of the protumoral properties of TAMs and MDSCs, a heterogeneous population including a granulocytic and a monocytic myeloid lineage, tumor cells actively recruit them via the secretion of chemotactic factors such as *CCl2*, *Csf1* and *GM-CSF* (Condeelis & Pollard, 2006; Cox et al., 2021; Pollard, 2004). These findings directed the interest in research on TAMs in TME, either ablating them or reprogram them towards an antitumorigenic M1 phenotype so probably enhancing therapy of pancreatic cancer. Inter alia, Zhu et al. treated PDAC bearing mice with a *Csf1/Csf1R*-blockade. Finding a decrease in the total number of TAMs and a reprogramming to M1-like macrophage polarization. As a result, suggesting an improvement of immune checkpoint blockade (ICB) therapy given in a combinatorial treatment approach (Zhu et al., 2014). These promising results also found in an early Phase I clinical study. Unluckily the treatment failed in a Phase II clinical trial to improve the progression free survival of PDAC patients (Bear et al., 2020). Hence, further studying myeloid cell sustained immunosuppression and gaining a deeper understanding of TAMs also under treatment conditions is worth focusing on.

1.4. Mouse models of PDAC

As a preclinical model, mouse models of cancer play an important role in adapting the pathobiology from human PDAC *in vivo*. Thereby, being able to study the connection of genetic alterations with the onset and progression of the tumor as well as to examine therapy efficacy. Furthermore, getting insight into the interplay of tumor cells with the stromal compartment with its composition of immune cells. The development of genetically engineered mouse models (GEMM) provides organ specific tumor models that resemble tumor progression and histopathological features. In PDAC, endogenous expression of *KRAS*-mutation, predominant in pancreatic cancer, induces the initiation of pancreatic intraepithelial neoplasia (PanIN) and their progression to invasive and metastatic diseases. Inducible oncogenic *Kras*^{G12D} expression is achieved by a Cre-recombinase under the control of a pancreas specific promotor like *Pdx-1* or *Ptf1a*, flanked by a constructed *Lox-STOP-Lox* (LSL) cassette upstream of the *Kras* locus (Hingorani et al., 2003; Jackson et al., 2001). Further development done resulted in the generation of a next-generation PDAC model with a dual-recombinase system using a *Flp*-recombinase under a *Pdx-1* promoter (*Pdx-1-Flp*) aiming at the feasibility of more comprehensive genetic remodeling (Schönhuber et al., 2014). In addition, the usage of murine orthotopic implantation models giving the chance to investigate reproducible PDAC cell lines *in vivo*. Thus, being preferentially used for therapeutic approaches (Mallya, Gautam, Aithal, Batra, & Jain, 2021; Schmitt, Saur, Bärthel, & Falcomatà, 2022). Taking advantage of all the information given by mouse experiments a versatile approach is needed. Hence, using flow cytometry to study the cellular composition (Spitzer et al., 2017), image analysis of PDAC tissue like immunofluorescent imaging to preserve the phenotype and localization of cells (Tsujikawa et al., 2017) and scRNA-seq as a high resolution method to assess the transcriptional profiles and cellular states (Bärthel et al., 2023; Tirosh et al., 2016). Summarized, this approach enables us to gain numerous features of tumor and stromal cells and to get a better understanding of the great complexity of the immune

compartment in the TME including its intra- and intercellular communication (Binnewies et al., 2018).

1.5. Objectives of this work

Till today, PDAC is a lethal disease with an unfavorable prognosis and short survival times. Compared to other cancer entities it contains a unique stromal compartment with a predominance of immunosuppressive TAMs interfering with therapeutical strategies. Despite great efforts done, the exact features of TAM subpopulations, the reason for their protumoral potential and the possibility of a successful reprogramming *in vivo* remain unclear. For this reason, this work is focusing on following questions:

- i. Do distinct TAM subpopulations differ in their proportion in endogenous GEMMs and molecular subtypes of orthotopic implanted PDAC?
- ii. Which functional subpopulations of TAMs can be revealed in PDAC subtypes on single cell level?
- iii. Are there changes in TAM frequency and subpopulations upon combinatorial drug treatment of PDAC?

The objective of this work is to further characterize the heterogeneous TME landscape in PDAC focusing on TAMs. Therefore, using GEMMs and orthotopic implanted mouse models in a versatile approach with immunofluorescent imaging, flow cytometry and scRNA-seq analysis. By further characterizing TAM features *in vivo* detecting potential points of attack and at long last allowing a more effective therapy of pancreatic cancer.

2. MATERIALS

This chapter includes all materials I used myself for experiments and analysis.

2.1. Mouse PDAC cell lines

The mouse PDAC cell lines I used in my experiments were generated in the research groups of Prof. Dieter Saur and Prof. Günter Schneider. Subsequent cell lines, used in my experiments, were further characterized and published by Müller et al. with big contribution of the research group of Prof. Roland Rad (Mueller et al., 2018):

PDAC subtype	Cell line No.
Classical C2b	8442
Classical C2b	8661
Mesenchymal C1	9091

2.2. Antibodies

2.2.1. Multi-colour Confocal Microscopy

Application	Manufacturer	Specificity	Cat.number/RRID
IF: 1:150	Bio-Rad	CD68	Cat#MCA1957GA, RRID:AB_324217
IF: 1:300	Thermo Fisher	iNOS	Cat#PA1-036, RRID:AB_325773
IF: 1:300	Abcam	CD80	Catalog-No. ab254579
IF: 1:300	Thermo Fisher	Arg1	Cat#PA5-85267, PRID:AB_2792410
IF: 1:300	Abcam	Mannose receptor	Cat#ab64693, RRID:AB_1523910
IF: 1:200	Biotium	F-Actin	Catalog-No.00046-T; CF633 Phalloidin
IF : 1:200	Thermo Fisher	Secondary anti-rat	Cat#A- 21209,RRID:AB_2535795
IF : 1:200	Thermo Fisher	Secondary anti-rabbit	Cat#A- 11034,RRID:AB_2576217

2.2.2. Multi-colour Flow cytometry

Application	Manufacturer	Specificity	Cat.number/RRID
FACS: 1:100	BD Biosciences	CD4 BUV805 (Clone GK1.5)	Cat#564922; RRID:AB_2739008
FACS: 1:20	BD Biosciences	CD3 ϵ BUV395 (Clone 145-2C11)	Cat#563565; RRID:AB_2738278
FACS: 1:30	BD Biosciences	CD11c BUV737 (CloneHL3)	Cat#564986; RRID:AB_2739034
FACS: 1:25	BD Biosciences	NK1.1 BUV395 (Clone PK136)	Cat#564144; RRID:AB_2738618
FACS: 1:100	BD Biosciences	Siglec-F BB515	Cat#564514; RRID:AB_2738833
FACS: 1:100	Biologend	CD8a BV785 (Clone 53-6.7)	Cat#100749;RRID:AB_11218801
FACS: 1:100	Biologend	CD45 PerCP Cy5.5 (Clonel3/2.3)	Cat#147705; RRID:AB_2563537
FACS: 1:100	Biologend	CD19 FITC (Clone &D%)	Cat#115505; RRID:AB_313640
FACS: 1:200	Biologend	EpCAM APC/AF647 (CloneG8.8)	Cat#118212; RRID:AB_1134101
FACS: 1:200	Biologend	Ly6C BV785 (Clone HK1.4)	Cat#128041; RRID:AB_2565852
FACS: 1:100	Biologend	CD11b BV650 (Clone M1/70)	Cat#101239;RRID:AB_11125575
FACS: 1:30	Biologend	F4/80 BV650 (Clone BM8)	Cat#123131;RRID:AB_10901171
FACS: 1:200	Biologend	Ly6G PE (Clone1A8)	Cat#127607; RRID:AB_1186104
FACS: 1:20	Biologend	CD68 APC-CY7 (Clone FA-11)	Cat#137023; RRID:AB_2616812
FACS: 1:50	Biologend	CD25 BV650 (Clone PC61)	Cat#102038; RRID:AB_2563060
FACS: 1:50	Biologend	TCR γ/δ BV421 (Clone GL3)	Cat#118120; RRID:AB_2562566
FACS: 1:500	Biologend	CD62L PE (Clone MEL-14)	Cat#104408; RRID:AB_313095

FACS: 1:30	Biolegend	CD44 APC/Fire750 (Clone IM7)	Cat#103062; RRID:AB_2616727
FACS: 1:100	Biolegend	TruStain FcX CD16/32 (Clone93)	Cat#101320; RRID:AB_1574975
FACS: 1:100	Biolegend	TER-119/Erythroid Cells BV421	Cat#116233; RRID:AB_10933426
FACS: 1:20	Biolegend	CD45 APC/AF647 (Clone 30F11)	Cat#103124; RRID:AB_493533
FACS: 1:20	Biolegend	CD31 APC/AF647 (Clone 390)	Cat#102416; RRID:AB_493410

2.3. Mediums and reagents

Product	Manufacturer
Aceton	Sigma
Anti-donkey Serum	Sigma
Anti-goat Serum	Sigma
Bovine Serum Albumin (BSA)	Sigma
DAPI (4',6-Diamidino-2-Phenylindole, dihydrochloride)	Biotium
DMEM high glucose	Sigma
Eosin Y Solution, 0,5%	Sigma
Ethanol (100%)	Merck
Ethanol (80%)	BrüggemannAlcohol
Fetal calve serum (FCS)	Sigma
Hematoxylin, Mayer's (Lilie's Modification)	Agilent
Phosphate buffered saline (PBS)	Sigma
Roti® Histofix 4%	Carl Roth GmbH
Tissue-Tek O.C.T compound	Sakura Finetek
Triton® X-100	Merck KGaA
Vectashield® mounting medium for immunofluorescence	Vector Laboratories

2.4. Kits

Product	Manufacturer	Catalog No.
Agilent High Sensitivity DNA Kit	Agilent	#5067-4626
Chromium Chip B Single Cell Kit, 16 rxns	10x Genomics	#1000074
Chromium i7 Multiplex Kit, 96 rxns	10x Genomics	#120262
Chromium NextGEM Chip G Single Kit, 48 rxns	10x Genomics	#1000120
Chromium Next GEM Single Cell 3' GEM, Library & Gel Bead Kit v3.1, 16 rxns	10x Genomics	#1000121
Chromium Single Cell 3' GEM, Library & Gel Bead Kit v3, 4 rxns	10x Genomics	#1000092
Dead cell removal kit, mouse	Miltenyi Biotec	#130-090-101
Debris removal kit, mouse	Miltenyi Biotec	#130-109-398
Dual Index Plate TT Set A	10x Genomics	#3000431
Library Construction Kit, 16 rxns	10x Genomics	#1000190
Tumor dissociation kit, mouse	Miltenyi Biotec	#130-096-730
Zombie Aqua Fixable Viability Kit	Biologend	#423102

2.5. Software and databases

Software version	Reference	URL/Producer
CellRanger (v3.1.0)	n.a.	https://support.10xgenomics.com/single-cell-gene-expression/software (10x Genomics)
FlowJo (v10.8.1)	n.a.	FlowJo LLC, Ashland, OR, USA
GraphPad Prism (v8)	n.a.	GraphPad Software, Inc.
Image Scope (v12.3)	n.a.	Leica Biosystems, Wetzlar
Leiden (v0.8.1)	(Traag, Waltman, & van Eck, 2019)	https://github.com/vtraag/leidenalg

Python (v3.8.3)	n.a.	https://www.python.org (Python Software)
Scanpy (v1.8.1)	(Wolf, Angerer, & Theis, 2018)	https://github.com/theislab/scanpy
UMAP (v0.4.6)	(Becht et al., 2018)	https://github.com/lmcinnes/umap

3. METHODS

3.1. Animal experiments

All experiments including animal studies were performed fulfilling the requirements of the European guidelines for the care and the use of laboratory animals and were approved by local authorities of the Technical University of Munich (TUM) as well as the Regierung von Oberbayern.

3.1.1. Mouse strains

To achieve tissue-specific overexpression of genes in the pancreas and expression of mutated alleles the *Cre-loxP* system (Orban, Chui, & Marth, 1992) was applied. Hence, two mouse strains were interbred. One expressing a Cre recombinase under control of a tissue-specific promoter and the other one carrying the transgene, or the mutated allele silenced by a translational stop element flanked by *loxP* sites (LSL) (Hingorani et al., 2003). The deletion of the stop cassette and tissue-specific expression of the relevant gene in the descendants occurred because of the recombination of the *loxP* sites by the Cre recombinase. Subsequent genotype was used in this study:

Genotype group	Allele sequence
PK	<i>Ptf1a^{Cre/+}, LSL-Kras^{G12D/+}, Pdx1-Flp, FSF-Kras^{G12D/+}</i>

And following mouse strains were used:

Mouse strain	Allele name	Reference
Ptf1atm1(cre)Hnak	<i>Ptf1a^{Cre/+}</i>	(Nakhai et al., 2007)
Krastm4Tyi	<i>LSL-Kras^{G12D/+}</i>	(Hingorani et al., 2003; Jackson et al., 2001)
Krastm1Dsa	<i>FSF-Kras^{G12D/+}</i>	(Schönhuber et al., 2014)
Tg(Pdx1-flpo)#Dsa	<i>Pdx1-Flp</i>	(Schönhuber et al., 2014)

3.1.2. Mouse genotyping and dissection

Each mouse got an explicit ear marking at the age of 2 to 3 weeks for later identification. DNA was extracted from the ear punches.

If the mouse developed a pancreatic tumor, an approximately 3-4 mm tumor piece was taken for isolation of a tumor cell line and measurements (weight and size of the tumor) were taken. A piece of the pancreatic tumor was fixed for 1.5-2 hours for cryo sections (3.4.1), the rest of the organ collection (pancreas, spleen, stomach, intestine, liver, lung, heart and kidneys) was fixed overnight in 4% Roti® Histofix. Genotyping and dissection of mice was mainly conducted by Dr. Stefanie Bärthel and Dr. Chiara Falcomatà.

3.1.3. Orthotopic implantation of PDAC cells in mice

For orthotopic implantation mice with a C57BL/6 background were used and isolated pancreatic tumor cells were cultured in tumor cell medium. 2500 to 10000 cells diluted in D-MEM were orthotopically injected into the pancreas. Orthotopic implantations were performed by Dr. Stefanie Bärthel, Dr. Chiara Falcomatà, Jack Barton and Saskia Ettl. (Falcomatà et al., 2022)

3.1.4. Nintedanib and Trametinib treatment of tumor bearing mice

Orthotopic implantation of tumor cell lines were conducted as described in 3.1.3 into the pancreas of C57Bl/6J mice. Randomization of mice was done when the tumor size was approximately 100mm³. For the treatment of tumor bearing mice the following drugs were used: Nintedanib (dosage 50 mg/kg, 5 days a week applied with oral gavage) and Trametinib (dosage 3 mg/kg, 5 days a week applied with oral gavage). One week after implantation of tumor cells mice were scanned with magnetic resonance imaging (MRI) and sacrificed after completion of the treatment. Treatment of mice was performed by Dr. Chiara Falcomatà together with Dr. Stefanie Bärthel. (Falcomatà et al., 2022)

3.2. Histopathological analysis of PDAC cohort

Sample collection as well as H&E staining was mainly done by Dr. Chen Zhao (E. Zhao et al., 2021). The histopathological analysis of the H&E samples was performed by pathologist Prof. Moritz Jesinghaus. The stromal compartment in the H&E sections was analyzed in up to 2 slides per PDAC sample.

3.3. Flow cytometry analysis of innate and adaptive immune cells

For fluorescence-activated cell sorting part of the mouse pancreas was taken and transferred into cold PBS on ice. To avoid dying of cells the following steps were carried out quickly and time of the tissue lying on ice was kept as short as possible. For mincing and enzymatically digesting the tissue a dissociation kit (Milteny Biotec) was used with agitation for 40 minutes at 37°C. The digested and minced tissue meshed through a 100µm mesh, next spun down and then resuspended in cold PBS with 2% FCS. To discriminate live from dead cells and to identify immune cells for each sample 100 µl of a solution containing Zombie Aqua Fixable Viability Kit (Biolegend, 1:500) and anti-mouse CD16/CD32 FC block (Biolegend, 1:100) were prepared, added into the wells and stained on ice for 10 minutes in the dark. After washing the cell solution with PBS the following antibody cocktail was added to label immune cells: CD4 BUV805 (BD, 1:100), CD3εBUV395 (BD, 1:20), CD8a BV785 (Biolegend, 1:100), CD45 PerCP Cy5.5 (Biolegend, 1:100), CD19 FITC (Biolegend, 1:100), EpCAM APC/AF647 (Biolegend, 1:200) for acquisition of adaptive immune cells; CD11c BUV737 (BD, 1:30), NK1.1 BUV395 (BD, 1:25), Ly6C BV785 (Biolegend, 1:200), CD11b BV650 (Biolegend, 1:100), F4/80 BV421/PB (Biolegend, 1:30), CD45 PerCP Cy5.5 (Biolegend, 1:100),

Ly6G PE (Biolegend, 1:200), CD68 APC-CY7 (Biolegend, 1:20), EpCAM APC/AF647 (Biolegend, 1:200). After staining for 30 minutes, the sample preparation was completed by three washing steps in PBS with 2% FCS and centrifugation with 1500 rpm for 3 minutes and removal of the supernatant. Using the BD LSRFortessa™ 1,000,000 events were recorded per sample. Following, the flow cytometry data was analyzed with the FlowJo software (v10.6.2). The FACS analysis was done together with Dr. Stefanie Bärthel, Dr. Chiara Falcomatà and Jack Barton. (Falcomatà et al., 2022)

3.4. Immunofluorescence analysis of immune cells

3.4.1. Tissue fixation and tissue section

For cryo sections piece of PDAC tissue was fixed for 1.5-2 hours in 4% Roti® Histofix. Subsequent for dehydration the fixed tissue was transferred first into 15% sucrose for 4 hours and next to 30% sucrose overnight, both at 4°C. Afterwards the prepared tissue was embedded in Tissue-Tek® O.C.T.™ and moved to -80°C for long-term storing. In preparation of staining, series of 5µm thin slices were cutted using cryostat Leica CM3050 S. Until further use cutted tissue sections were stored at -20°C.

3.4.2. Antibody-based staining

For antibody-based immunofluorescent staining previously cutted sections were taken out of -20°C freezer, thawed in the incubator at 37°C for 1 minute and air dried at room temperature for 30 minutes. Then tissue was fixed with acetone for 6 minutes at 4°C and again air dried at room temperature for 30 minutes. Next sections were rehydrated in PBS for 10 minutes. Following, a hydrophobic pen was applied around the tissue drawing a closed ring. Next, the section was incubated in 100µl of blocking solution (10% anti-goat serum and 10% anti-donkey serum in PBS) in a humid chamber for 1 hour. For addressing macrophage subpopulations 50 µl of a solution of primary antibodies diluted in 3% BSA together with 6% TritonX in PBS was given up the sections for 3 hours in a humid chamber: rat anti-CD68 (Bio-Rad, 1:150), respectively with rabbit anti-Arg1 (Thermo Fisher, 1:300), rabbit anti-Anti-Mannose Receptor (Abcam, 1:300), rabbit anti-iNOS (Thermo Fisher, 1:300) or rabbit anti-CD80 (Abcam, 1:300). Next, tissue sections were washed 3 times for 5 minutes in PBS and then incubated with secondary antibody goat anti-rabbit 488 (Invitrogen, 1:200) or donkey anti-rat 594 (Invitrogen, 1:200) diluted in PBS for 1 hour. After 3 times washing in PBS for 5 minutes nuclei were counterstained with DAPI (Biotium, 1:1000) for 10 minutes. After washing again 3 times for 5 minutes in PBS cryo sections were mounted with Vectashield® mounting medium and stored at 4 °C until performing image analysis. Previously described steps following the tissue fixation with acetone were all performed at room temperature and steps following the incubation with primary antibodies were all done in the dark.

3.4.3. TAM imaging with confocal microscope

PDAC tissue of respective mice was taken and tissue sections were stained as described in 3.4.2. For macrophages CD68 was used as whole lineage marker. M1-like macrophages were stained using iNOS or CD80 and M2-like macrophages using Arg1 or CD206 (Arlaukas et al., 2018; Bertani et al., 2017; Xue, Yan, Zhang, & Xiong, 2018). At least 3 mice per genotype and 5 fields of view of the tumor core as well as the tumor invasive front were imaged by Leica TCS SP8 Confocal Laser Scanning Microscope with a 40x-oil and 63x-oil objective.

3.4.4. TAM counting with ImageJ

After imaging the PDAC sections with the confocal microscope macrophages were counted using the ImageJ software. Therefore, dividing all CD68 positive cells through all cells showing a positive nuclei-staining with DAPI. For quantifying macrophage subtypes the cells being positive for a subpopulation marker (Arg1, Anti-mannose receptor; iNOs or CD80) were divided through all cells positive for CD68. For each marker at least 3 mice per genotype and 5 fields of view were counted.

3.5. Single cell RNA sequencing

The steps performed in the following chapters 3.5.1 until 3.5.5 were mainly conducted by Dr. Stefanie Bärthel and Dr. Chiara Falcomatà.

3.5.1. Sample preparation

The following described steps were performed as described in Falcomatà et al.: “Tumor specimens were dissociated as described above. The cell suspension was strained through a 100 µm strainer, spun down and resuspended in 2% FCS/PBS including RNase inhibitor (NEB, #M0314L,1:100). Debris removal solution (Miltenyi #130-109-398) was used to remove cell debris from the dissociated tissue. Then the dead cell removal kit (Miltenyi #130-090-101) was used to enrich for live cells. The cell suspension was spun down and then resuspended in PBS and blocked for non-antigen-specific binding for 10 min on ice with anti-mouse CD16/CD32 FC block (Biolegend, 1:100). Cells were stained with the following antibodies for FACS sorting: TER-119 BV421 (Biolegend, 1:100), CD45-AF647 (Biolegend, 1:20), CD31-AF647 (Biolegend, 1:20) and EPCAM-AF647 (Biolegend, 1:20) for 30 min on ice. Cell sorting was performed using the BD FACS Aria Fusion. The sorted cells from the TER-119-negative/CD45-/CD31-/EPCAM-positive fraction (for enrichment of immune, endothelial and epithelial tumor cells and exclusion of erythrocytes) as well as TER-119-/CD45-/CD31-/EPCAM-negative fraction (for enrichment of fibroblasts/mesenchymal tumor cells and exclusion of erythrocytes). Sorted cells were collected in 2% FCS/PBS.” (Falcomatà et al., 2022)

3.5.2. Library preparation and sequencing

The library preparation as well as the sequencing were performed as described in Falcomatà et al.: “The sorted cells were counted, diluted in 2% FCS/PBS and up to 20,000 cells were loaded per lane on a 10x Chromium chip to generate gel beads in emulsion (GEMs). Single cell GEM Generation, barcoding and library construction was performed by using 10x Chromium Single Cell 3' v3 chemistry according to the manufacturer's instructions. cDNA and generated libraries were checked for sample size and quality on an Agilent TapeStation 4200 using DNA HS 5000 tape. Libraries were sequenced on the Illumina NovaSeq 6000 S2 (PE, 28+94 bp).” (Falcomatà et al., 2022)

3.5.3. Data pre-processing, integration and quality control

Likewise, the steps described in this section were conducted as described in Falcomatà et al.: “Alignment of the scRNA-seq data to the mouse reference genome (mm10, release 108.20200622), filtering, and barcode and unique molecular identifier counting was performed using the 10x Genomics Cell Ranger software (v3.1.0). The Python software package SCANPY was employed for all further analyses (v 1.6.0) (Wolf et al., 2018). Cells that expressed less than 200 genes or had more than 10% mitochondrial gene counts were excluded from the analysis. We also filtered out genes

with less than 20 counts. Counts were per-cell normalized and (log+1)-transformed. Highly variable genes were computed using either the first N=3000 most variable genes for the analyses across cell types, or tumor cells, and treatment conditions, the first N=800 genes when analyzing fibroblasts and the first N=2500 when analyzing T cells.” (Falcomatà et al., 2022)

3.5.4. Dimensionality reduction and clustering

Also, the dimensionality reduction, clustering as well as the annotation of cell types were done as described in Falcomatà et al.: “The Leiden algorithm (v0.8.1) (Traag et al., 2019) was used for cell clustering and Uniform Manifold Approximation and Projection (UMAP, v0.4.6) (Becht et al., 2018) for dimensionality reduction. The clusters were further annotated by assessment of known cell-type specific markers. Principal component analysis was performed with default parameters. Neighborhood graphs were computed based on n=10 principal components and k=30 neighbors and the calculation of all UMAP projections was based on default parameters. The optimal number of Leiden clusters was adjusted according to the sample of consideration.” (Falcomatà et al., 2022)

3.5.5. Gene Set Enrichment Analysis (GSEA)

Subsequent, the GSEA was done as written in Falcomatà et al.: “Differential gene expression analysis was performed using the tool `rank_genes_groups`, which is part of the SCANPY package (v1.6.0, <https://github.com/theislab/scanpy>). The Benjamini-Hochberg method was used to correct for multiple testing. Subsequent GSEA (Subramanian et al., 2005) was performed using GSEA v4.1.0 jar package and MSigDB v7.1 gene sets provided by Broad Institute, Massachusetts Institute of Technology and Harvard University. GSEA was conducted on a preranked gene list output of the differential gene expression analysis, genes were ranked based on “t test” metric. Parameters were set as follows: number of permutations was set to 1000 and enrichment statistic for scoring was set as “weighted”; other parameters were set as default. The cut-off for a significant FDR q-value was set at 0.25 and NOM p-value at 0.05.” (Falcomatà et al., 2022)

3.5.6. Cell-type-specific analysis of macrophages

The macrophage-cluster was determined due to the expression of CD68 and Lyz2, using the above-described quality-controlled and batch corrected data set (8,145 cells total). Different reference data sets (Kemp et al., 2021; L. Zhang et al., 2020; Zilionis et al., 2019) were used to determine subclusters of macrophages and monocytes. Wilcoxon rank-sum test was used to conduct differential gene expression analysis to distinguish monocyte and macrophage subclusters. Following, genes were rated (`log2fc_min=0.5`, `pval_cutoff=0.01`) and ‘MSigDB_Hallmark_2020’ gene set together with GSEAPy toolkit were used for gene set enrichment analysis.

4. RESULTS

As oncogenic *KRAS* is known to be the key driver mutation leading to the initiation of PDAC formation, hereby resembling the human disease, I focused on models containing this pathway for my study. Beneath oncogenic signaling, there is growing evidence for the great leverage of the immunosuppressive TME on tumor progression and the success of or the resistance to therapeutic strategies (Falcomatà, Bärthel, Schneider, Saur, & Veltkamp, 2019; Ruffell & Coussens, 2015; Schneider, Schmidt-Supprian, Rad, & Saur, 2017). Moreover, the unraveled molecular subtypes of PDAC (classical and mesenchymal) are suggested to deeply influence intratumoral characteristics. Thus, our lab investigated a novel combinatorial treatment combining the MEK-inhibitor Trametinib and the multi-kinase inhibitor Nintedanib, comparing the before defined molecular subtypes in a reproducible model of orthotopic implanted PDAC. Our results indicate the effectiveness of the combinatorial therapy especially in the mesenchymal subtype and in part a reprogramming of the immunosuppressive TME accompanied by its sensitizing to ICB by *PD-L1* inhibition was recently published (Falcomatà et al., 2022). Additionally, our results showed a difference in the tumor cell expression of *Ccl2* and *Csf1* comparing the classical and mesenchymal subtype. As these secreted factors are known to attract TAMs and MDSCs to the local TME enhancing their immunosuppressive features it pushes us to further characterize the TME in untreated as well as treated mouse models of PDAC, in this work focusing on the myeloid cell compartment.

In case colleagues or collaborators contributed to the results submitted in this study it is marked in the chapter methods.

The TME of PDAC harbors a tremendous range of immune and stromal cells. This spotlights the complex landscape of this cancer type. Given that, we hypothesize intra- and intertumoral heterogeneity in endogenous *Kras*^{G12D}-driven PDAC.

In addition, the molecular subtypes of PDAC (classical and mesenchymal) deeply influence tumor characteristics and affect tumor progression. Thus, we hypothesize differences in their TME composition in particular dimension concerning the myeloid cell compartment.

In both approaches we aim to (i) characterize the composition of the immune compartment focusing on myeloid cells, (ii) identify potential differences in TAM polarization status and (iii) reveal distinct subclusters of TAMs and uncover their anti- and protumoral properties on single cell level.

We pursued these aims through a multimodal approach using fluorescent imaging by Confocal Microscopy, flow cytometry and scRNA-seq. Therefore, taking advantage of a in our lab previously generated endogenous *Kras*^{G12D}-driven PDAC model (PK) and a cohort of an orthotopic implantation model of PDAC with previously generated and deeply characterized cell lines of the classical and mesenchymal subtype.

By that, we were able to address TAM subpopulations at multiple ways.

4.1. Multimodal approach reveals inter- and intratumoral heterogeneity of the myeloid cell compartment in *Kras*^{G12D}-driven PDAC

First, I aimed to get a deeper understanding of the TME composition of PDAC *in vivo* using a GEMM resembling the tumor progression and histopathological features of the human disease. In the Saur lab, a large cohort of 500 tissue samples (FFPE) from mouse PDAC containing distinct genetic alterations was previously acquired. This cohort was gathered by Dr. Chen Zhao and after H&E staining underwent histopathological analysis by Prof. Moritz Jesinghaus. Beside the tumor grading, also the stromal compartment and the immune cell infiltration were evaluated. Among these the PK group, solely containing oncogenic *Kras*^{G12D}, showed the highest intra-group heterogeneity with a stromal content differing from 5 up to 70%. Thus, for my study I focused on this mutagenic group.

Being able to systematically characterize the immune cell infiltration into the TME understanding its features we implemented a multimodal approach of multi-colour Confocal Microscopy, multi-colour flow cytometry and scRNA-seq after harvesting the tumor tissue of PDAC bearing mice.

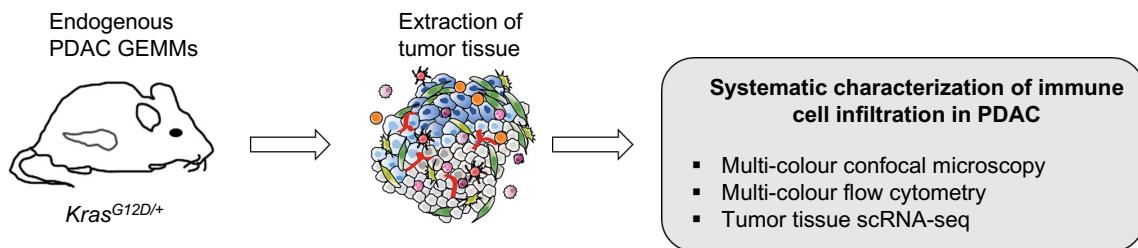


Figure 1 Overview of experimental workflow for a systematic analysis of the TME of endogenous *Kras*^{G12D}-driven PDAC

Scheme for systematic analysis of the PDAC TME using *Kras*^{G12D/+}-driven GEMMs. Tumor tissue was isolated when mice reached the human endpoint. Then, PDAC immune cell infiltration was analyzed by multi-colour confocal microscopy, multi-colour flow cytometry and tumor tissue scRNA-seq.

Illustration of the graph by courtesy of Chiara Falcomatà

Immune cell characterization by flow cytometry using an antibody-based staining panel for the assessment of innate and B-/T-cell immune clusters of our PK tumors exhibited besides neutrophils, macrophages to be the largest immune population (**Figure 2 A**). Beyond this, our sorting results reveal great intertumoral heterogeneity regarding the amount of macrophage infiltration driving us to define two distinct cohorts being called TAM high (>3% macrophages) and TAM low (<0,8% macrophages) (**Figure 2 B and C**). In this small cohort we were not able to define corresponding differences concerning the T-cell cohort nor significant differences in survival (**Figure 2 C and D**). Perhaps, studying T-cell subpopulations in a larger amount of tumor samples would unravel such distinctions.

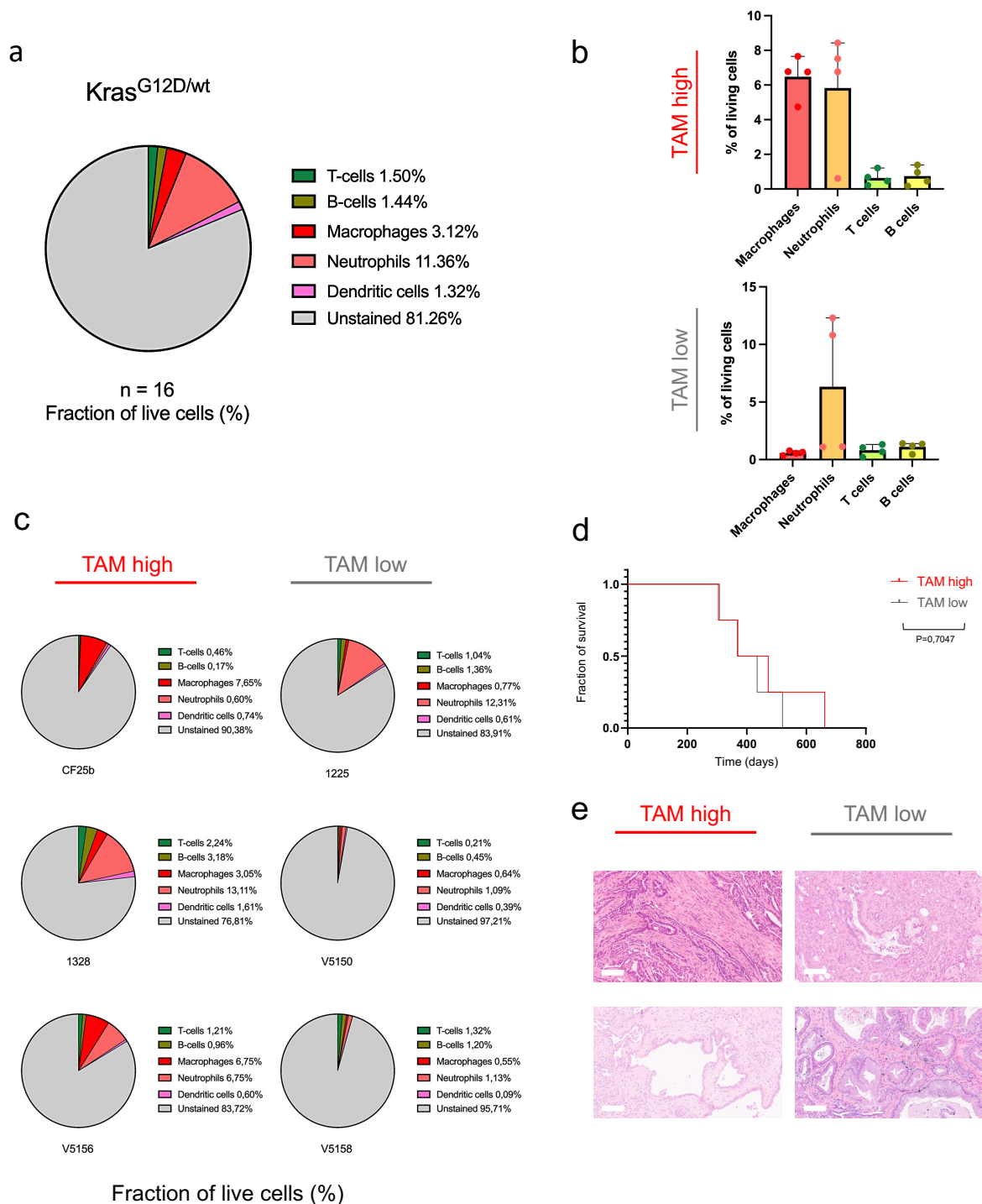


Figure 2 Characterization of immune cell infiltration in *Kras*^{G12D}-driven PDAC

a, Endogenous *Kras*^{G12D}-driven PDAC tissues (n=16) were dissociated and analyzed by flow cytometry. Pie chart represents fractions of innate and adaptive immune cell infiltration of living cells in tumor tissue.

b, Bar chart depicts percentage of macrophages, neutrophils, T cells and B cells of living cells analyzed by flow cytometry. The box plots representing the mean value and scatter, individual tumors are shown as single points. TAM high meaning tumors with over 3% and TAM low tumors with under 0,8% TAM infiltration.

c, Pie charts showing fraction of immune cell infiltration of representative PDAC samples with high TAM infiltration and low TAM infiltration. At least 3 tumors were quantified per chart.

d, Kaplan-Meier survival curve of mice bearing endogenous *Kras*^{G12D}-driven PDAC showing no significant difference between the two groups. P-value was calculated by student's Log-rank-Test. At least 4 mice per group were analyzed.

e, Representative H&E staining TAM-high and TAM-low cohort of endogenous tumor samples. Scale bars, 100 μ m.

Because of the found differences in our flow cytometry data concerning the macrophage population, being in particular interested in characteristics of the different TAM cohorts, we implemented an antibody-based staining panel for immunofluorescent imaging. Macrophages are known to express diverse cell surface as well as intracellular receptors, of them CD68 is often used as a pan-lineage marker in mouse and human samples (Boutillier & ElSawa, 2021; Gordon et al., 2014; Kuninaka et al., 2022). Especially in a tumor context, this diverse population is present in different polarization subsets. Of them, the classical M1-like macrophages displaying pro-inflammatory features like iNOS (Nos2), which activity is increased after stimulation with IFN δ and leads to the production of NO an inflammatory mediator involved in pathogen defense (Boutillier & ElSawa, 2021; Kuninaka et al., 2022). In addition, the surface expression of CD80 on macrophages is often used to determine its M1-polarization status (Mahon, Kelly, McCarthy, & Dunne, 2020). In contrast, the alternatively activated M2-like macrophages are defined by immunosuppressive features as the expression of Arg1, an enzyme depleting the amino-acid L-Arginine from the TME, thereby dampen Ag-specific T-cell response (Arlauckas et al., 2018; Rodriguez et al., 2004). A second marker typically expressed by M2-like macrophages is the Mannose-receptor Mrc1 (CD206) (Gordon et al., 2014; Jaynes et al., 2020).

Concordant with our finding in the flow cytometry data quantification on fluorescent antibody stained PDAC slides for the constitutive macrophage marker CD68 in comparison to all cells with a positive nuclear staining using DAPI confirmed a TAM high and a TAM low cohort (**Figure 3 A**). To address distinct TAM subpopulations in these groups we performed co-staining of the M1-polarization markers iNOS or CD80 and the M2-polarization markers Arg1 or Mrc1 respectively with the pan-lineage marker CD68. Subdividing the co-stained cells through all CD68⁺ cells indicated considerable higher M2 signatures of TAMs over all PDAC samples, but no significant differences between the TAM high and the TAM low cohort comparing their M1- and M2-polarization status (**Figure 3 B and C**).

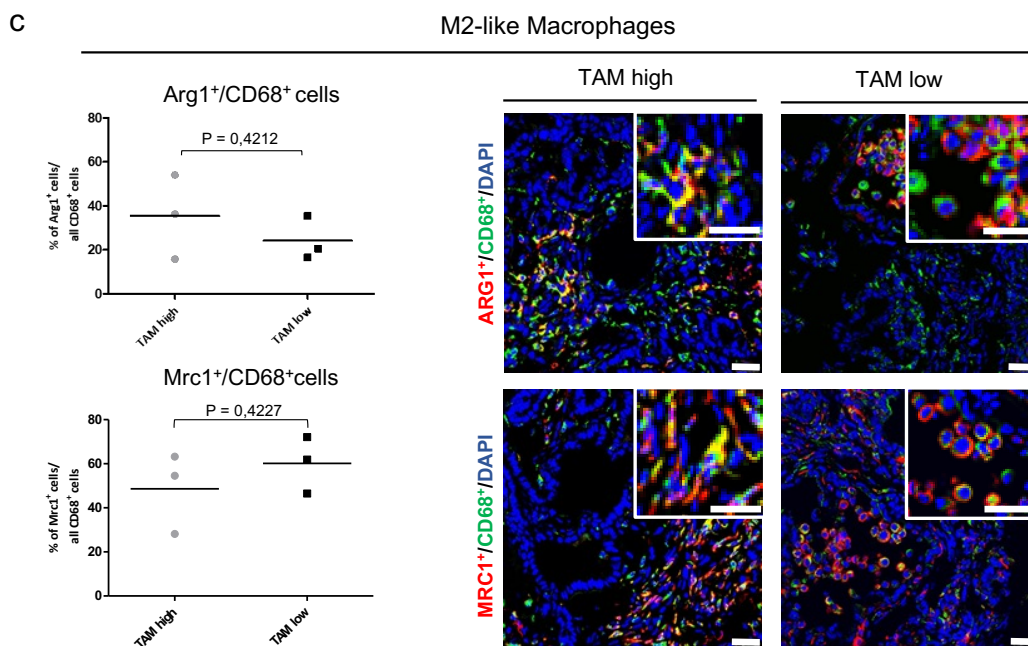
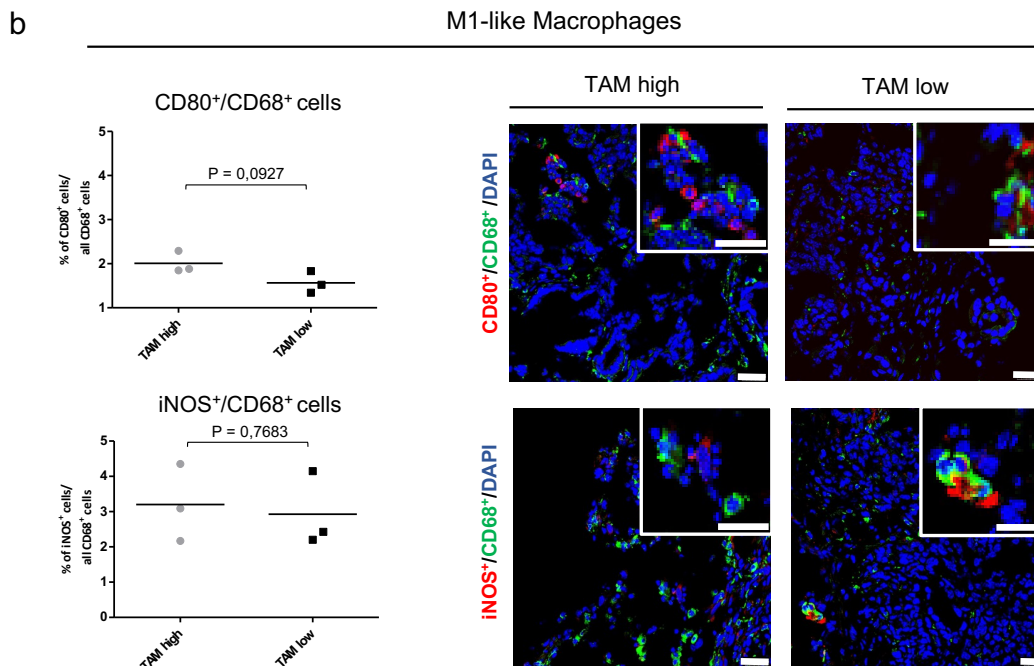
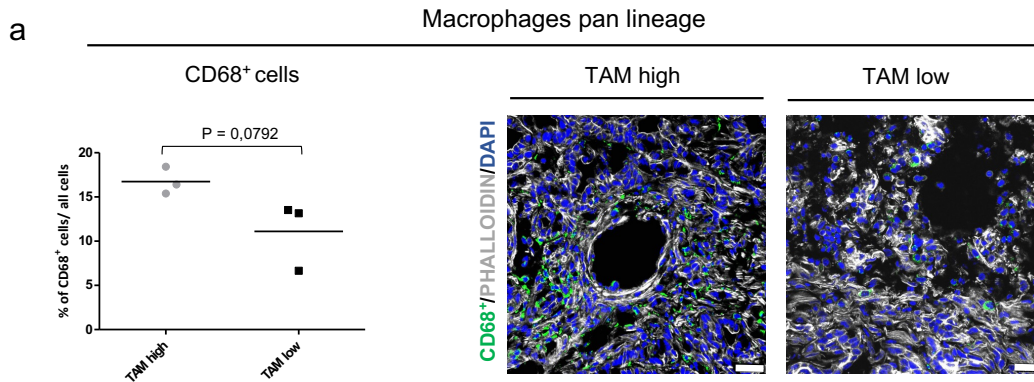


Figure 3 Identification of macrophage subpopulations in endogenous *KRAS*^{G12D}-driven PDAC by immunofluorescence

a, Left, Quantification of macrophage pan lineage marker CD68 in TAM high and TAM low PDAC (identified by flowcytometry) by immunofluorescence staining. P-value was calculated by student's t-test. **Right**, representative images of tissue sections stained for CD68 (green), Phalloidin (grey) was used for staining of actin filaments and DAPI (blue) for nuclear staining. Scale bars, 25 μ m.

b, Left, Quantification of M1-like macrophage polarization markers CD80 and iNOS of CD68-positive cells in TAM high and TAM low PDAC (identified by flowcytometry) by immunofluorescence staining. P-value was calculated by student's t-test. **Right**, representative images of tissue sections stained for CD80 or iNOS (red), CD68 (green) and DAPI (blue) for nuclear staining. Scale bars, 25 μ m.

c, Left, Quantification of M2-like macrophage polarization markers Arg1 and Mrc1 of CD68-positive cells in TAM high and TAM low PDAC (identified by flowcytometry) by immunofluorescence staining. P-value was calculated by student's t-test. **Right**, representative images of tissue sections stained for Arg1 and Mrc1 (red), CD68 (green) and DAPI (blue) for nuclear staining. Scale bars, 25 μ m respectively 50 μ m in the upper right pictures.

Note: At least 3 tumors and 5 fields of view per TAM group were counted.

Predominance of an immunosuppressive myeloid cell population including TAMs is a key feature of the TME in PDAC. Respecting the rising evidence that the crosstalk in the TME drives this versatile immune population to adopt a variety of protumoral characteristics and that the M1-/M2-polarization states are just two extremes in a broad range of TAM phenotypes, we applied scRNA-seq analysis to tumors selected of our *Kras*^{G12D}-driven PDAC (PK) cohort. Thus, giving us the chance to study the whole transcriptome of individual cells free of any anticipated characteristics (Bärthel et al., 2023; Han, DePinho, & Maitra, 2021; Zilionis et al., 2019). After performing the scRNA-seq analysis of the tumor tissue, first the resulting library was pre-processed and then integrated in the SCANPY environment using BBKNN batch correction (Polański et al., 2020; Wolf et al., 2018). The received data set containing 7,186 cells was annotated by Leiden clustering due to common marker genes (**Figure 4 A**). To examine the functional subsets of myeloid cells we extracted them (2,572 cells) from the whole data set and subsequent repeated Leiden clustering.

On this basis 6 distinct monocyte/macrophage clusters could be classified. Among them we identified 3 macrophage clusters and 3 monocyte clusters including one monocyte subcluster expressing signatures of dendritic cells (DC), thus called MonoDC. Additionally, a separate DC cluster was found (**Figure 4 B**).

Differential gene expression analysis between these clusters (**Figure 4 C**) revealed the *Spp1*⁺ Monocyte cluster also highly expressed the immunosuppressive marker *Arg1*. Its eponymous marker *Spp1* was recently shown to be associated with an anti-inflammatory immunosuppressive phenotype in myeloid cells (Elyada et al., 2019; Katzenelenbogen et al., 2020). Besides that, the so called classical Monocyte cluster (Zilionis et al., 2019) highly expressed *Ccr2* which was shown to support the extravasation of tumor cells in a mouse model of breast cancer (Qian et al., 2011). The corresponding chemokine *Ccl2* is highly secreted by many tumor types to attract monocytes to the TME and shape them towards tumor promoting cells (Kalbasi et al., 2017; Pollard, 2004).

Furthermore, the *Ccr2*⁺ Macrophage cluster displayed high levels of *Ccr2* and HLA-associated genes like *H2-Aa* and *Cd74*, thus resembling a TAM subpopulation described by Kemp et al. appearing in early stages of pancreatic cancer and getting progressively lost in advanced disease stages. The *C1q*⁺*Ccr2*⁺ and the *C1q*⁺*Cd74*⁺ Macrophage clusters are both characterized by high expression of the complement factors *C1qa/b* and *c*. A complement-high TAM subpopulation, additionally expressing HLA-associated marker genes as well as markers of an alternative activation status like *Mrc1*, was also recently identified by Kemp et al. (Kemp et al., 2021). The complement cascade is a crucial mediator of innate immunity its upregulation in TAMs was shown to favor tumor growth (Roumenina et al., 2019) and suggested to help

PDAC cells circumvent complement-mediated cell death in a TAM-dependent manner (R. Zhang et al., 2019). Taking a look at the marker gene expression for TAM ontogeny compared to other groups our two *C1q*⁺ Macrophage clusters showed preferential TR features (**Figure 4 E**). Next, comparing the mean expression of marker genes of the myeloid cell compartment in a model of lung cancer given by Zilionis et al. to our defined monocyte/macrophage group (**Figure 4 D**) showed that our classical Monocyte cluster exhibits the transcriptional state of so-called “classical monocytes” being able to extravasate and evolve into macrophages or DCs in tissues, whereas our *Spp1*⁺ Monocytes preferentially express markers of so-called “non-classical monocytes” suggested to mainly stay in the vasculature patrolling its walls (Zilionis et al., 2019). All 3 found macrophage clusters showed mixed signatures of M1/M2 polarization with a predominance of M2-like marker genes especially in our *C1q*⁺ Macrophage clusters (**Figure 4 F and G**).

Interestingly, the highest expression of hypoxia-induced factors naming *Arg1* and *Nos2* competing for L-Arginine as their substrate, both being able to sustain suppression of T-cell activity, (Colegio et al., 2014; Doedens et al., 2010) and *Vegfa* involved in neovascularization, thereby contributing to tumor progression and extravasation, (Veglia et al., 2021) were exhibited by our *Spp1*⁺ Monocytes (**Figure 4 F**).

Figure 4 scRNA-seq reveals distinct subpopulations of TAMs in endogenous *Kras*^{G12D}-driven PDAC

a, Left, UMAP plot displaying Leiden clustering of identified cell subpopulations of one *Kras*^{G12D}-driven PDAC (ID=1328). 7186 cells were sequenced. Macrophages/monocytes cluster is highlighted. Right, dot plot showing mean expression of marker genes used for identification of cell subpopulations.

b, UMAP plot showing extracted macrophages/monocytes cluster revealing 7 distinct subclusters of tumor infiltrating myeloid cells. 2572 cells were further analyzed.

c, Differential gene expression analysis showing top 4 expressed genes for each identified cluster of tumor-infiltrating myeloid cells (TIM) in a heatmap.

d, Heatmap depicts reference marker genes by Zilionis et al., 2020 used for identification of distinct subpopulations of TIMs. Scale bar shows mean expression per group.

e, Heatmap displaying mean marker gene expression characteristic for different macrophage ontogeny (marker genes for tissue resident and bone marrow derived origin). Scale bar shows mean expression per group.

f, Heatmap showing mean expression of marker genes characteristic for M1- and M2-like macrophage polarization. Scale bar shows mean expression per group.

g, UMAP plots displaying expression of 4 representative polarization marker genes (left: M1-like marker genes *Cd80* and *Nos2*; right: M2-like marker genes *Arg1* and *Mrc1*).

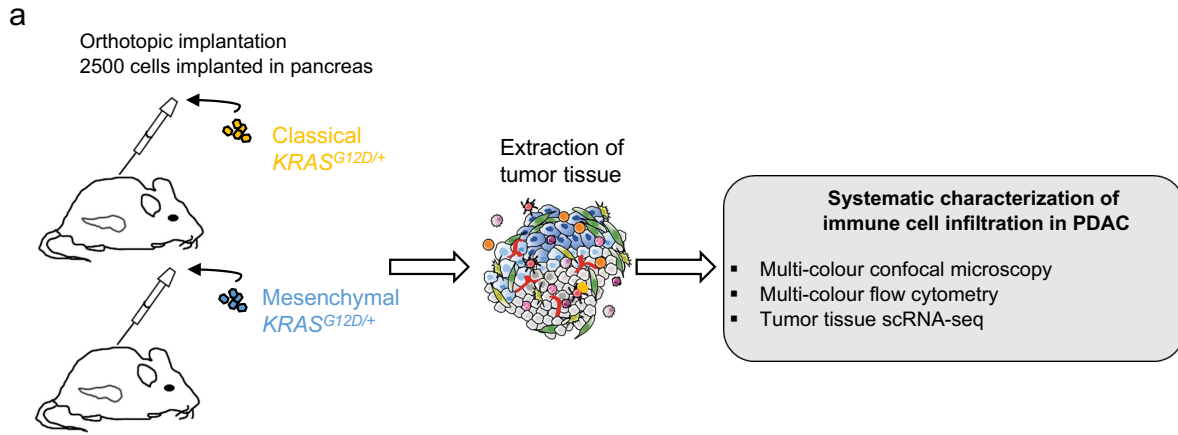
Clustering analysis was done by Stefanie Bärthel.

Taken together, our results concerning the monocyte/macrophage population in the cohort of endogenous *Kras*^{G12D}-driven PDAC sustained the picture of a predominance in protumoral signatures of TAMs in the TME, beyond that displaying great inter- as well as intratumoral heterogeneity. Especially our *Spp1*⁺ and *C1q*⁺ Monocyte and Macrophage clusters elucidated key pathways of their immunosuppressive gene profiles.

4.2. Different molecular PDAC subtypes display considerable distinctions in their myeloid cell compartment

The classical and mesenchymal subtypes were defined as the two major groups of human PDAC and known to impact tumor progression and even therapy response (Bärthel et al., 2023; Falcomatà et al., 2023; Moffitt et al., 2015). These findings directed our interest to potential differences in the TME closely related to the distinct tumor cell subtypes. Being able to study and compare the immune cell infiltration in both subgroups we used an orthotopic implantation model injecting our well-characterized PK cell lines of the classical (n=2 lines) or mesenchymal (n= 1 line) subtype into the pancreas of our syngeneic immunocompetent C57Bl6/J mice (Mueller et al., 2018). After the development of a macroscopic tumor, we harvested the tumor tissue for a multimodal approach including multi-colour Confocal Microscopy, multi-colour flow cytometry and scRNA-seq analysis (**Figure 5 A**). This allowed us to study special features of the TME in a reproducible and well-defined model.

Comparing cell type proportions between our classical and mesenchymal tumors we found a considerable difference in the abundance of myeloid cells. Corresponding between the innate panel of our flow-cytometry data (**Figure 5 B**), our quantification results of the tissue slides stained with the macrophage pan-lineage marker CD68 (**Figure 5 C**) and our scRNA-seq analysis (**Figure 5 D**) we found a remarkable higher infiltration of monocytes and macrophages in our mesenchymal tumor samples, whereas our classical tumor samples were higher in neutrophils.



PDAC subtype	Classical	Mesenchymal
Cell line ID	8442 8661	9091

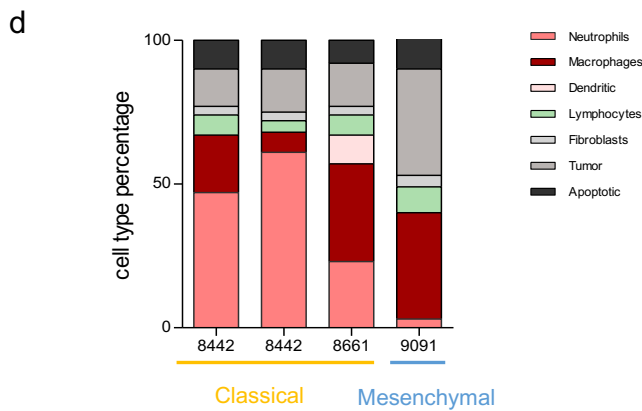
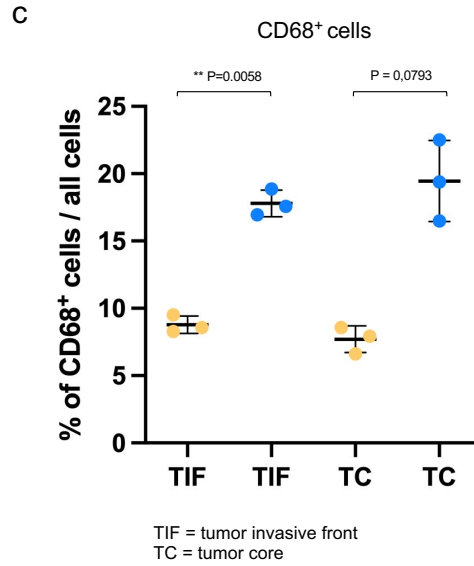
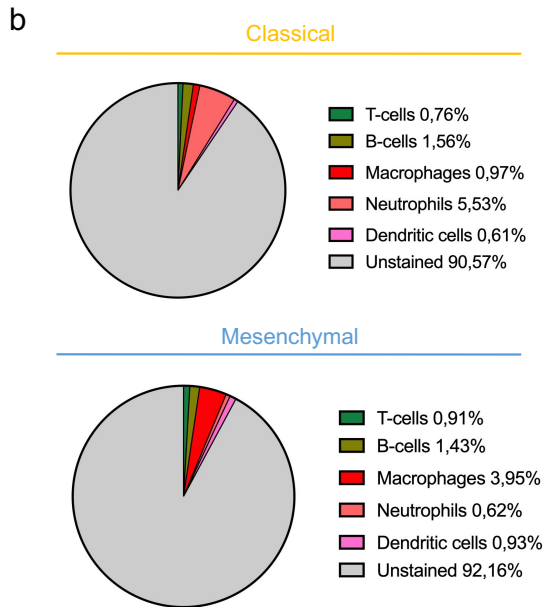


Figure 5 TME characterization in orthotopically implanted PDAC of classical and mesenchymal cell lines

a, Schematic representation of experimental workflow: Orthotopic implantation of 2500 classical (8442, 8661) or mesenchymal (9091) PDAC-cells in the pancreas tail of syngeneic immunocompetent C75B16/J mice. Organ collection after development of a macroscopic tumor. Analysis of immune cell infiltration by multi-colour confocal microscopy, multi-colour flow cytometry and tumor tissue scRNA-seq.

Illustration of the graph by courtesy of Chiara Falcomatà.

b, Pie charts comparing flow cytometry data of immune cell infiltration in classical and mesenchymal PDAC samples.

c, Quantification of macrophage pan lineage marker CD68 in classical and mesenchymal PDAC cohort (identified by flow cytometry). P-value was calculated by student's t-test.

d, Innate and adaptive immune cells counted as percentage of all living cells in scRNA-seq results of classical and mesenchymal PDAC samples.

Note: At least 3 samples were analyzed per group and in C at least five fields of view for each sample were counted. P-value of performed t-test named above counting results.

Corresponding all three analysis (B-D) show a higher TAM infiltration in mesenchymal tumor samples.

Recognizing these differences in the myeloid cell compartment we got interested in distinctions concerning the macrophage polarization status between both transcriptional PDAC subtypes. To address this concern, we applied the antibody-based staining panel already implemented on our endogenous GEMMs (see chapter 4.1., Figure 3) on tissue slides of both, the classical and mesenchymal, lines. In addition to the above-described significant higher TAM infiltration in mesenchymal compared to classical tumors counting all CD68⁺ cells (**Figure 6 A**), we discovered a predominance of M2-polarization in macrophages over all samples, counting the M2-like markers Arg1 and Mrc1 (**Figure 6 C**) in comparison to the M1-like markers iNOS and CD80 (**Figure 6 B**). Moreover, we found a tending but not significant higher M2-like macrophage signature in the mesenchymal PDAC subtype.

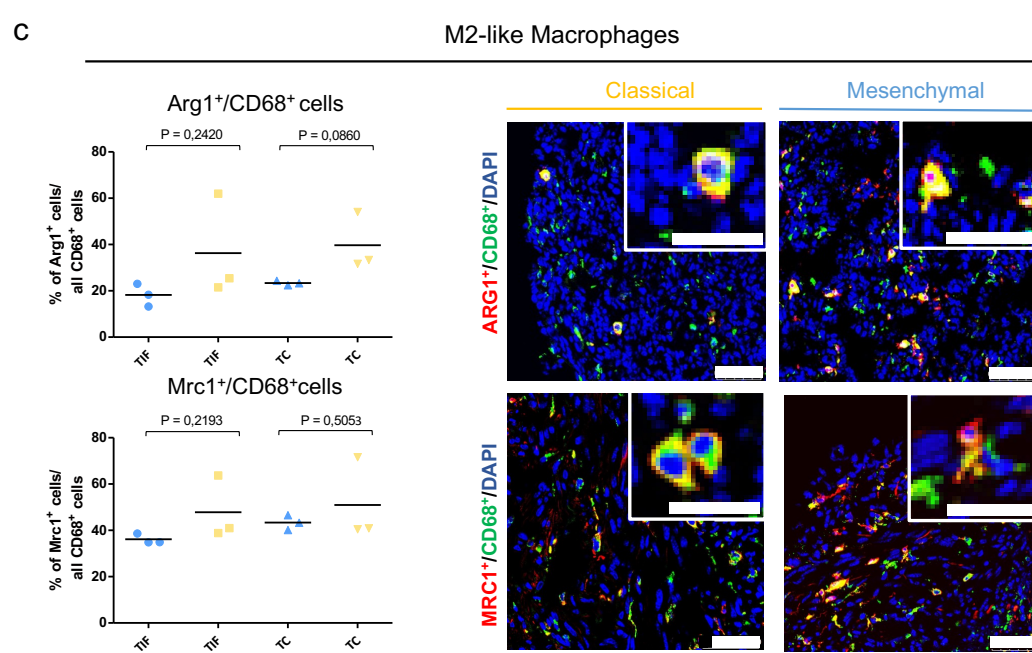
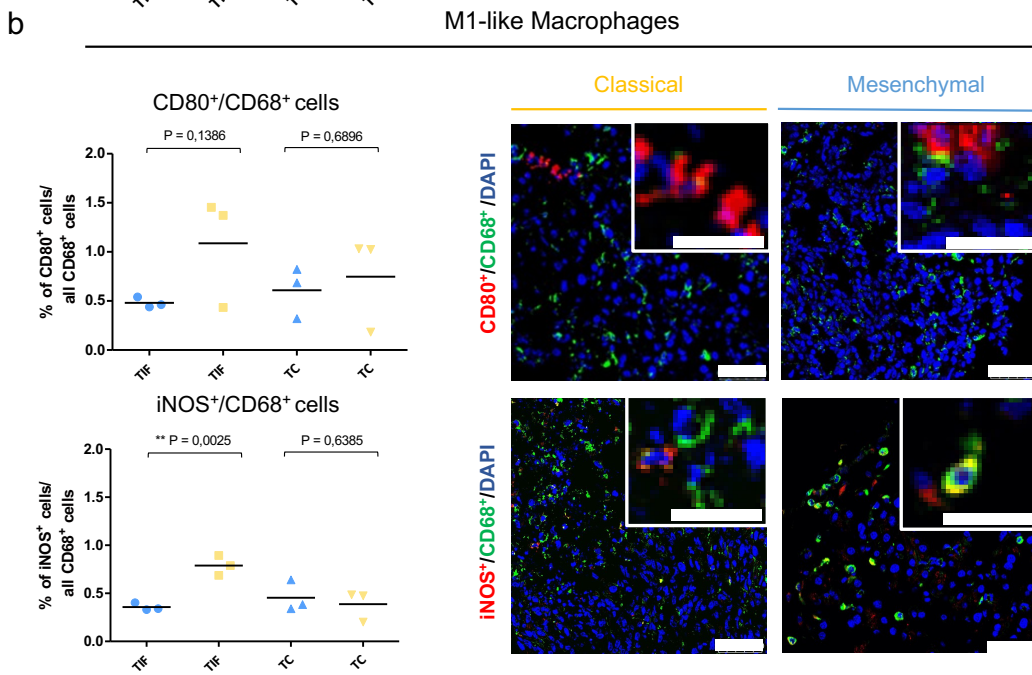
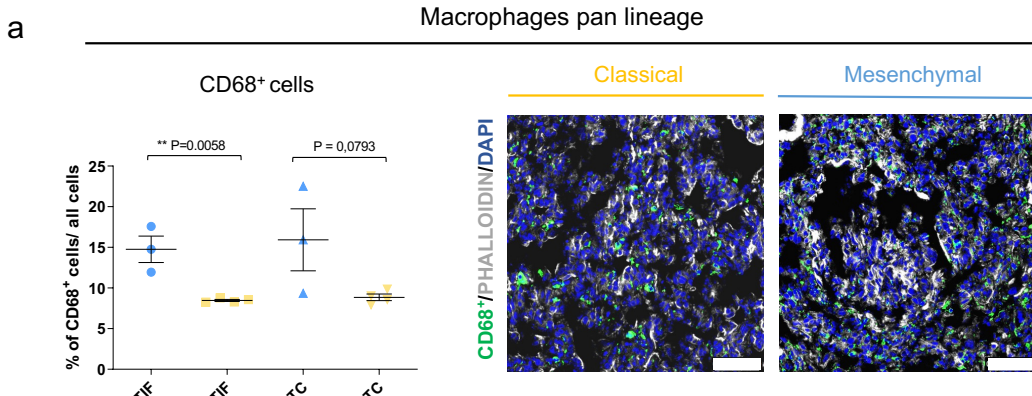


Figure 6 Identification of macrophage subpopulations in transcriptional PDAC subtypes by immunofluorescent imaging

a, Quantification of macrophage pan lineage marker CD68 in the tumor invasive front (TIF) and the tumor core (TC) from immunofluorescent staining representative depicted right. Phalloidin used to stain actin filaments and show shape of tumor cells. Counting results showing higher TAM infiltration in tumors derived from mesenchymal cell line (consistent to results of FACS analysis and scseq data depicted in F5B). P-value of performed t-test above quantification results.

b, Quantification of M1-like macrophage polarization markers in the TIF and the TC. Counting CD80⁺/CD68⁺- and iNOS⁺/CD68⁺-cells (double stained). Representative pictures of immunofluorescent staining shown right.

c, Quantification of M2-like macrophage polarization markers in the TIF and the TC. Counting Arg1⁺/CD68⁺- and Mrc1⁺/CD68⁺-cells (double stained). Representative pictures of immunofluorescent staining depicted right.

Counting results indicating higher infiltration of M2-like macrophages compared to M1-like counting results in B, in classical as well as mesenchymal tumor samples.

Note: At least 3 tumors and 5 fields of view per subtype and TAM group were counted. P-values of performed t-tests are shown above quantification results left. Scale 25 μ m, respectively 50 μ m, in the pictures in top right corner.

Given this assertive M2-polarization of TAMs in our PDAC model we wanted to get a deeper insight in their immunosuppressive features. Hence, we performed scRNA-seq analysis for both transcriptional subtypes (classical n = 2 lines, mesenchymal n = 1 line). As for our scRNA-seq data of the endogenous PDAC sample presented in chapter 4.1., our generated libraries were pre-processed and integrated in the SCANPY environment using BBKNN batch correction (Polański et al., 2020; Wolf et al., 2018). The resulting data set, containing 7,329 cells, was next supplied to Leiden clustering and the found clusters were annotated due to common marker genes (**Figure 7 A and B**).

As described above comparing the cell type proportions of the immune cell compartment revealed a remarkable higher infiltration of myeloid cells, in particular monocytes and macrophages, in the mesenchymal compared to the classical PDAC subtype (**Figure 5 D**).

To further investigate the phenotype of the myeloid cells we extracted them from the total scRNA-seq data and reclustered the resulting data (774 cells) using Leiden clustering.

Our findings elucidated 5 distinct functional subsets accordingly 3 monocyte clusters, including a MonoDC cluster (monocytes showing gene signatures of DCs), and 2 macrophage clusters naming *C1qc*⁺ Macrophages and *Spp1*⁺ Macrophages (**Figure 7 C**). We performed differential gene expression analysis between these clusters. The *C1qc*⁺ Macrophages displayed, besides its eponymous markers of the complement cascade *C1qa/b* and *c*, the highest expression of the immunosuppressive markers *Mrc1* (C. Lee et al., 2019) and *ApoE* (Revel, Sautès-Fridman, Fridman, & Roumenina, 2022). The *Spp1*⁺ Macrophage cluster displayed a high level of proangiogenic factors including *Vegfa*. (**Figure 7 D**)

Comparing the gene expression profiles of our monocyte/macrophage clusters to marker genes of myeloid cells given by Zilionis et al. revealed our *S100A8*⁺ Monocyte cluster resembles a monocyte subpopulation highly expressing neutrophil associated genes (**Figure 7 E**).

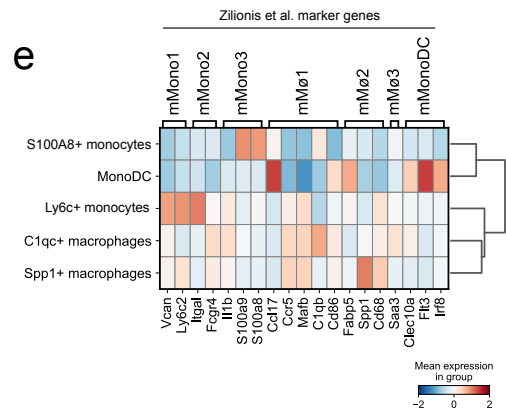
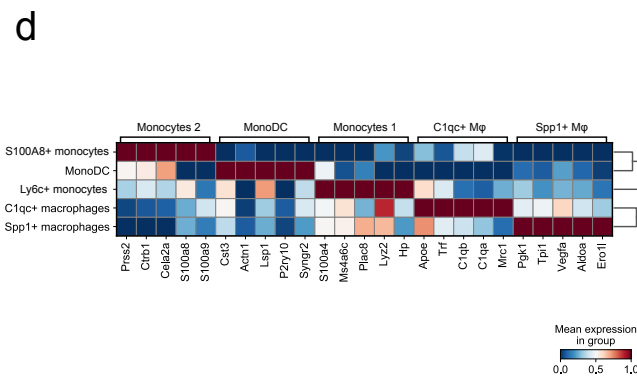
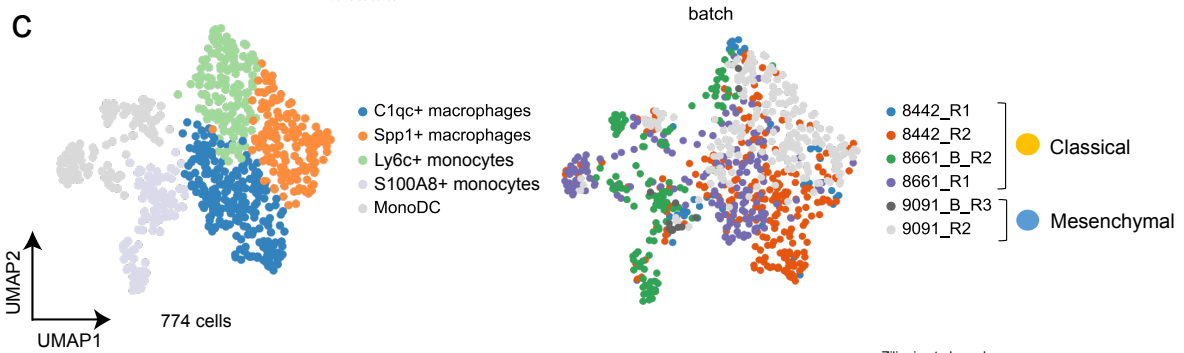
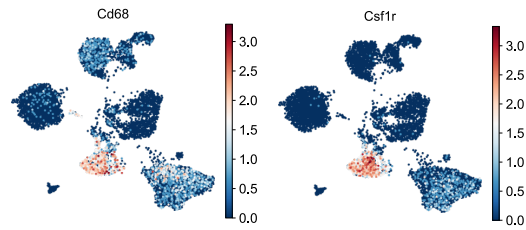
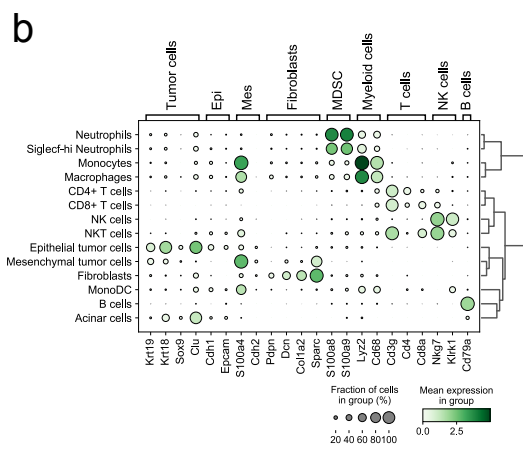
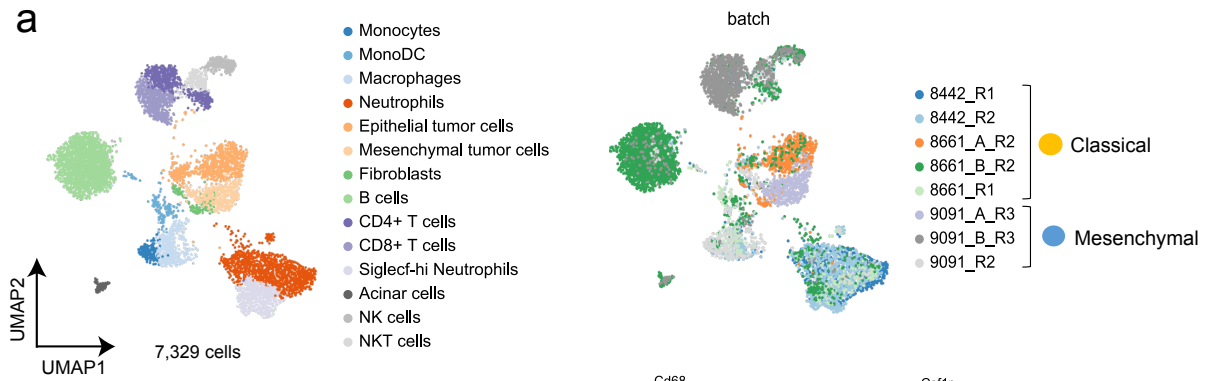


Figure 7 scRNA-seq analysis reveals distinct clusters of TIMs in classical and mesenchymal PDAC subtypes

- a**, Left, UMAP plots of displaying marker gene expression for adaptive and innate immune cells as well as classical and mesenchymal tumor cells identified with scRNA sequencing in transcriptional PDAC subtypes. Right, batch depicting contribution of classical subtype (8442, 8661) and mesenchymal subtype (9091) to the immune cell- and tumor cell- clusters. *Cd68* and *Csf1r* as markers representative for identification of macrophage clusters shown underneath.
- b**, Dot plot showing mean expression of markers used for identification of cell clusters.
- c**, Left, UMAP plot showing 9 distinct clusters of TIMs, including macrophage subpopulations, identified by scRNA-seq. Right, batch depicting contribution of classical subtype (8442, 8661) and mesenchymal subtype (9091) to distinct TIM-clusters.
- d**, Differential gene expression analysis showing the top 4 expressed genes for each identified TIM cluster in a heat map.
- e**, Identification of distinct TIM clusters. Analyzed marker genes according to Zilionis et al. 2020. Two representative markers depicted per cluster. Gene expression for *Spp1* shown mainly in macrophage cluster 2 and gene expression for *C1qc* mainly in macrophage cluster 1 and 8. Clustering analysis was done by Stefanie Bärthel.

Furthermore, being interested in the leverage of PDAC subtypes on the heterogeneity in the myeloid cell compartment we analyzed their contribution to the found subclusters. The mesenchymal line (9091) majorly contributed to our *Spp1*⁺ Macrophage cluster and our *Ly6c*⁺ Monocyte cluster. Whereas our both classical cell lines (8442 and 8661) to a larger amount contributed to our *S100A8*⁺ Monocyte and especially to our MonoDC cluster. Both, the mesenchymal as well as the classical subtype contributed to our *C1qc*⁺ Macrophage cluster (**Figure 8 A**).

Proceeded analysis of the outstanding marker genes for our macrophage clusters *Spp1*, shown to be associated with an immunosuppressive TAM phenotype, (Elyada et al., 2019; Katzenelenbogen et al., 2020) being highly expressed in our *Spp1*⁺ Macrophage cluster and at a much lower extent in our *C1qc*⁺ Macrophage and *Ly6c*⁺ Monocyte clusters. Whereas *C1qc* as part of the complement system, shown to be associated with a M2-like macrophage polarization (Kemp et al., 2021), was highly exhibited by our *C1qc*⁺ Macrophage cluster and in a smaller amount by our *S100A8*⁺ Monocyte cluster (**Figure 8 B**).

Looking for signatures of ontogeny we found our *C1qc*⁺ Macrophage cluster preferentially displays Tissue resident (TR) features (**Figure 8 C**).

Comparing the expression of M1-/M2-polarization gene profiles we found a predominance of M2-signatures over all 5 clusters and co-expression of pro- and anti-inflammatory signatures especially in our *C1qc*⁺ Macrophage cluster.

Moreover, the highest expression of hypoxia-induced factors *Arg1* and *Nos2*, competing partners in macrophage metabolism shown to interfere with T-cell activation, (Colegio et al., 2014; Doedens et al., 2010) and *Vegfa*, known to contribute to angiogenesis and invasiveness in PDAC, (Veglia et al., 2021) were exhibited by our *Spp1*⁺ Macrophage cluster (**Figure 8 D**).

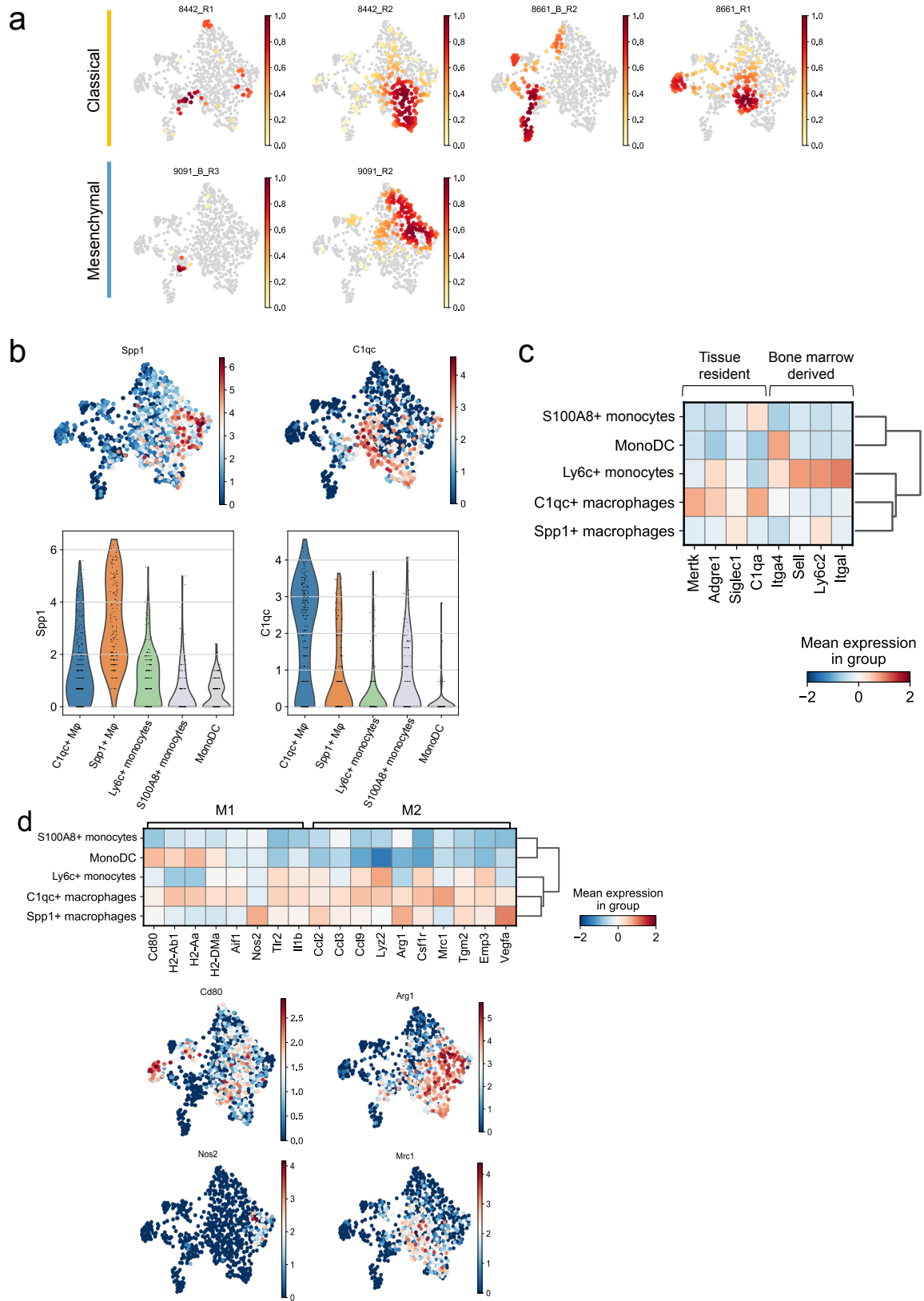


Figure 8 Identification of macrophage subclusters in molecular PDAC subtypes displaying distinct characteristics

a, Density plot showing contribution of classical (8442, 8661) and mesenchymal (9091) PDAC subtypes to different TAM clusters – highest density depicted in dark red. Classical subtype contributing preferentially to *C1qc*^{high} macrophage cluster and mesenchymal subtype preferentially to *Spp1*^{high} macrophage cluster.

b, Violin plots: left one showing amount of *Spp1* expression among TAM clusters and right one showing amount of *C1qc* expression among TAM clusters. Expression map of both markers depicted above. *Spp1* being preferentially expressed in macrophage cluster 2, whereas *C1qc* being preferentially expressed in macrophage cluster 1.

c, Identification of markers for distinct macrophage ontogeny. Heat map displaying mean expression of markers for tissue resident (TR) and bone marrow derived origin (BMD).

d, Heat map showing mean expression of markers characteristic for M1- and M2-like macrophage polarization. Indicating macrophage clusters with overlapping M1- and M2-like properties. Expression map of 4 representative polarization markers (left: *CD80* and *NOS2* for M1-polarized macrophages; Right: *Arg1* and *Mrc1* for M2-polarized macrophages) depicted underneath.

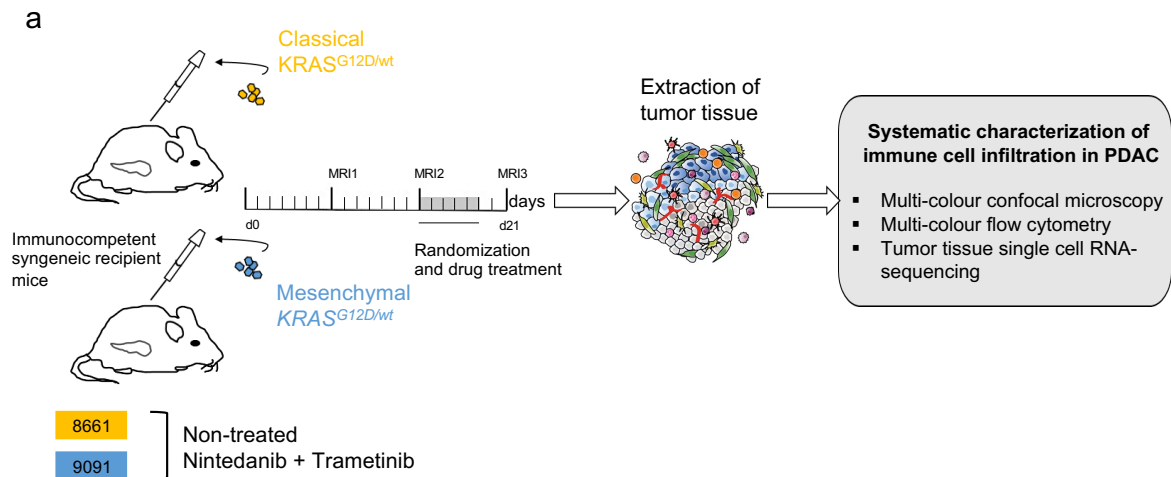
Clustering analysis was done by Stefanie Bärthel.

In summary, our analysis of the transcriptional PDAC subtypes in an orthotopic implantation mouse model revealed a predominance of immunosuppressive monocytes and macrophages in the mesenchymal subtype compared to the classical one. Our scRNA-seq data unveiled a *C1qc*⁺ Macrophage cluster with TR features originating from the classical as well as the mesenchymal tumor samples and a *Spp1*⁺ Macrophage cluster arising predominantly from the mesenchymal subtype.

4.3. Combinatorial drug treatment leads to an increase of proinflammatory features of TAMs

In our lab we aimed to address the great resistance of oncogenic *KRAS*-driven PDAC to therapy, especially in terms of ICB. Thus, we performed a high-throughput combinatorial drug screen. The result indicated the combination of the *MEK*-inhibitor Trametinib with the multi-kinase inhibitor Nintedanib as a promising pairing. We could show that the combinatorial treatment approach led to an increase of the infiltrating cytotoxic T-cells in our PDAC model. Thereby, sensitizing the aggressive mesenchymal subtype to ICB. These results were recently published in the research article “*Selective multi-kinase inhibition sensitizes mesenchymal pancreatic cancer to immune checkpoint blockade by remodeling the tumor microenvironment*” by Falcomatà, Bärthel et al. (Falcomatà et al., 2022).

Performing this study, we were also interested in further changes concerning the immune compartment occurring upon our combinatorial therapy (**Figure 9 A**). Our flow cytometry analysis showed higher macrophage infiltration in the mesenchymal compared to the classical tumor samples, but no numerous differences comparing the untreated control samples to the tumors of our combinatorial treatment cohort (**Figure 9 B and C**).



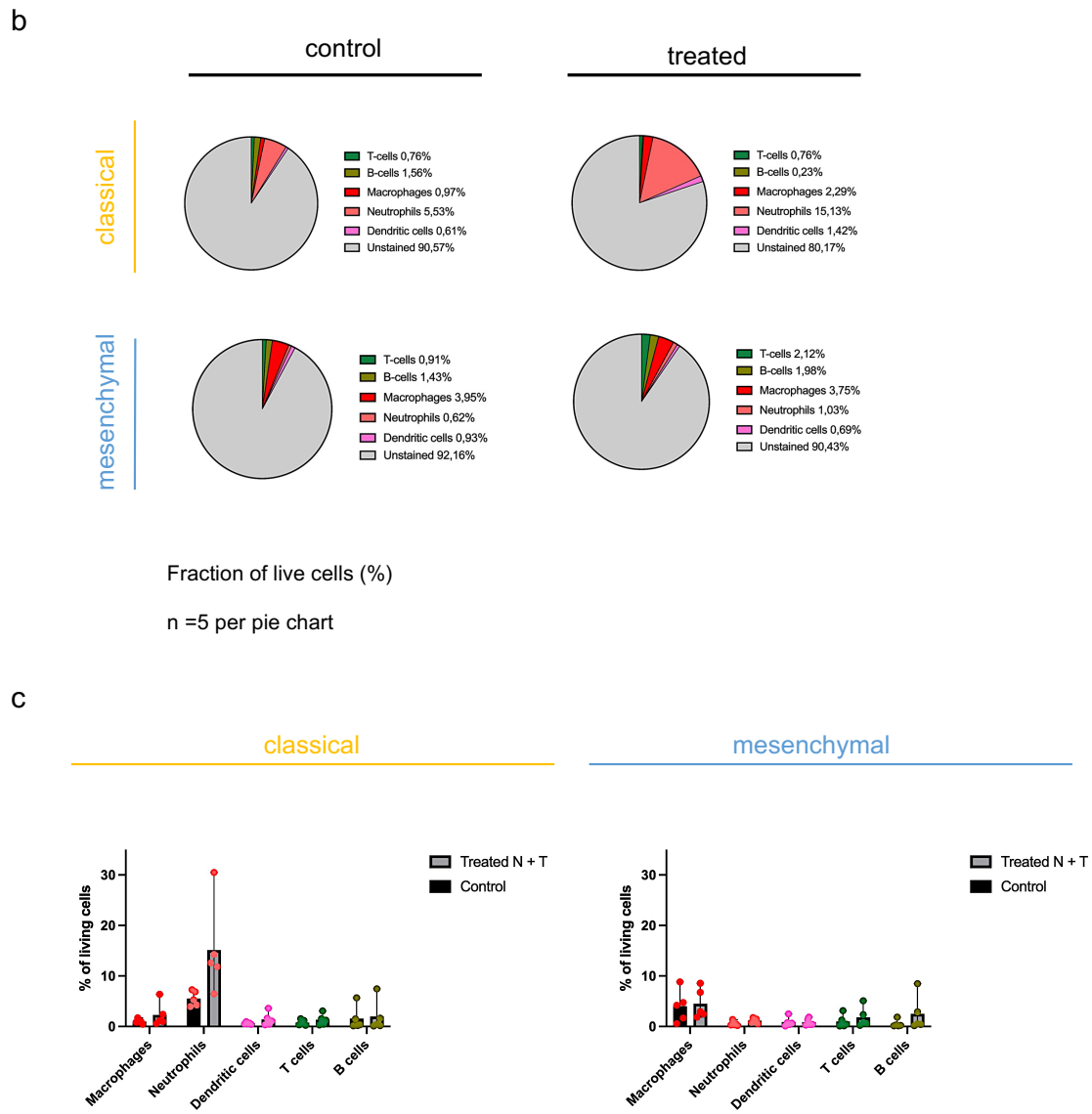


Figure 9 Characterization of TME in context of combinatorial drug treatment with Trametinib and Nintedanib of mice orthotopically implanted with *KrasG12D*-driven PDAC cell lines

a, Schematic representation of experimental workflow: Implantation of classical (8661) or mesenchymal (9091) PDAC cell line in pancreas tail of syngeneic immunocompetent C75Bl6/J mice, followed by imaging of the tumor growth by MRI one and two weeks after implantation. Subsequent start of daily drug treatment with Nintedanib and Trametinib for five days. Organ collection and analysis of the tumor tissue after third MRI at day 21. Analysis of immune cell infiltration by proceeding multi-colour confocal microscopy, multi-colour flow cytometry and tumor tissue scRNA-seq.

Illustration of the graph by courtesy of Chiara Falcomatà.

b, (left) Pie charts representing fraction of innate and adaptive immune cell infiltration into tumor tissue. Flow cytometry analysis of double treated tumor samples (Trametinib and Nintedanib) and (right) untreated control tumor samples of transcriptional PDAC subtypes, using the same classical (8661) and mesenchymal (9091) cell lines for implantation. Analysing 5 tumors per group. Comparison of FACS results between double-treated and untreated cohort showing no numerous difference in macrophage infiltration (illustrated in dark red).

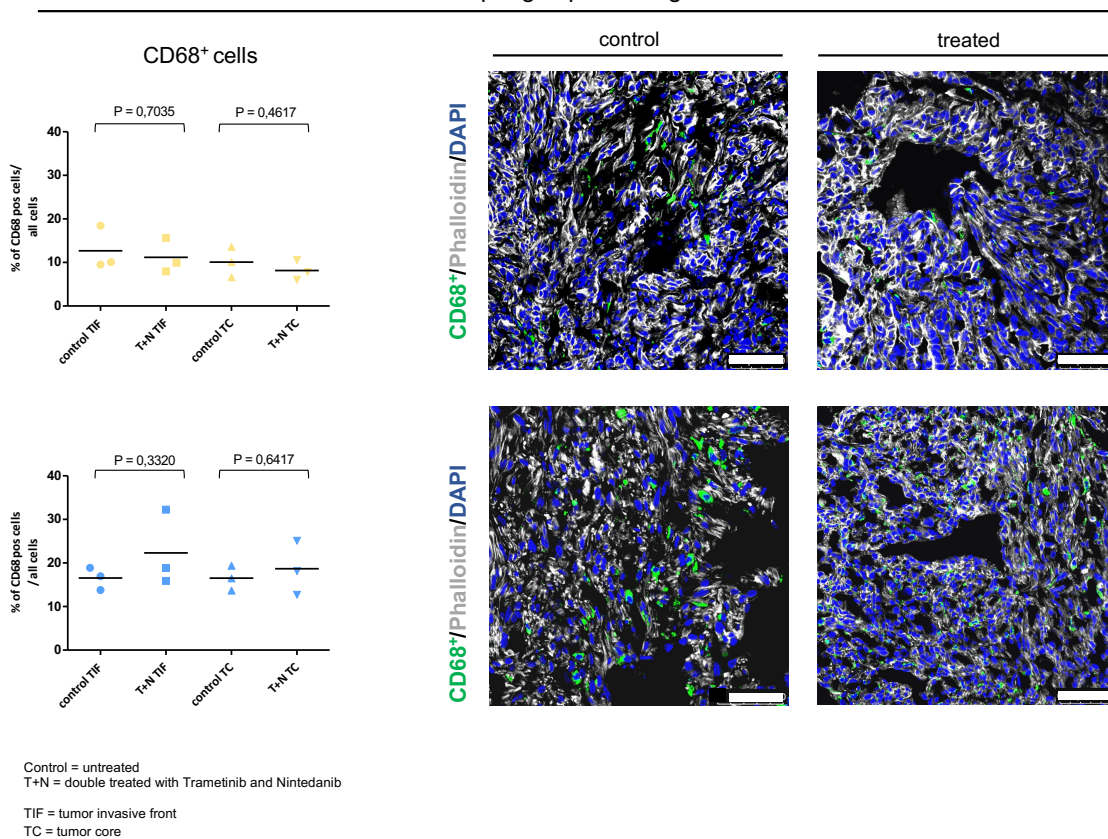
c, Comparison of immune cell infiltration in control- and treatment-samples of classical and mesenchymal tumor subtypes analyzed by flow cytometry and depicted in box plots. Showing higher macrophage infiltration into mesenchymal (right) tumor samples, but no numerous differences comparing macrophage infiltration in untreated and double-treated PDAC cohorts.

To further characterize potential changes of TAM polarization upon our combinatorial therapy we performed immunofluorescent staining, subsequent quantifying the imaged slides. The quantification of the macrophage pan-lineage marker CD68 confirmed the higher TAM infiltration in the mesenchymal compared to the classical PDAC subtype but showed likewise no substantial differences between our untreated control and our combinatorial treated cohort (**Figure 10 A**).

Moreover, the quantification of the macrophage subpopulation markers for M2-polarization Arg1 and Mrc1 showed a stable high expression of both markers after our combinatorial therapy (**Figure 10 C**), whereas the results for iNOS and CD80 indicated a tendency towards an increase of these M1-polarization markers (**Figure 10 B**). (Falcomatà et al., 2022)

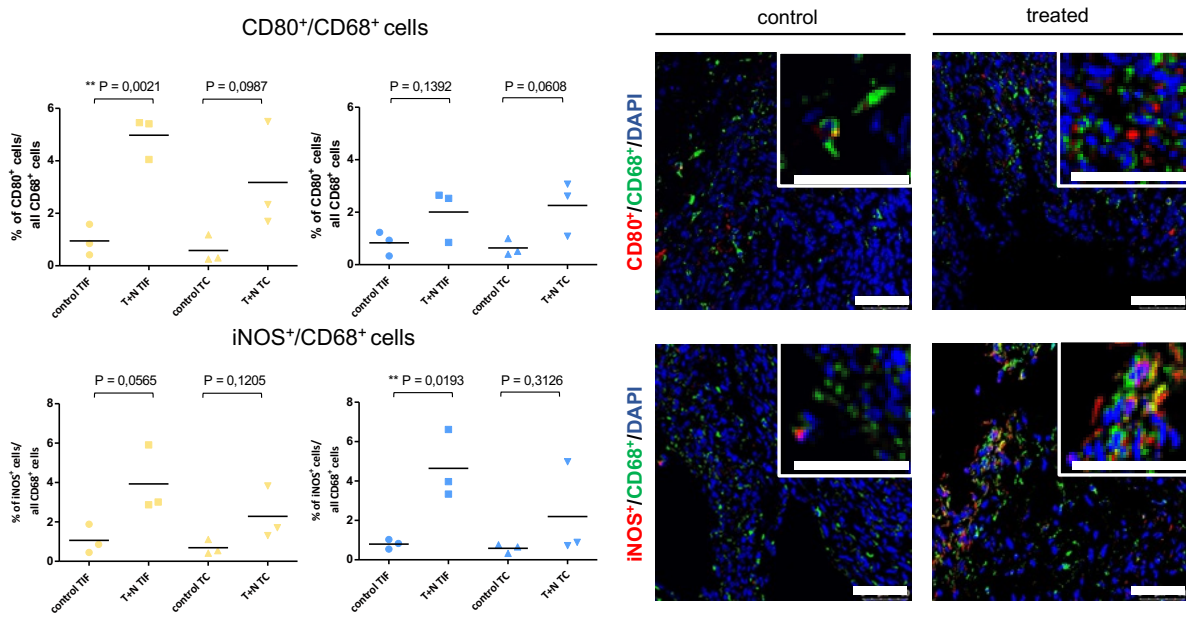
a

Macrophages pan lineage



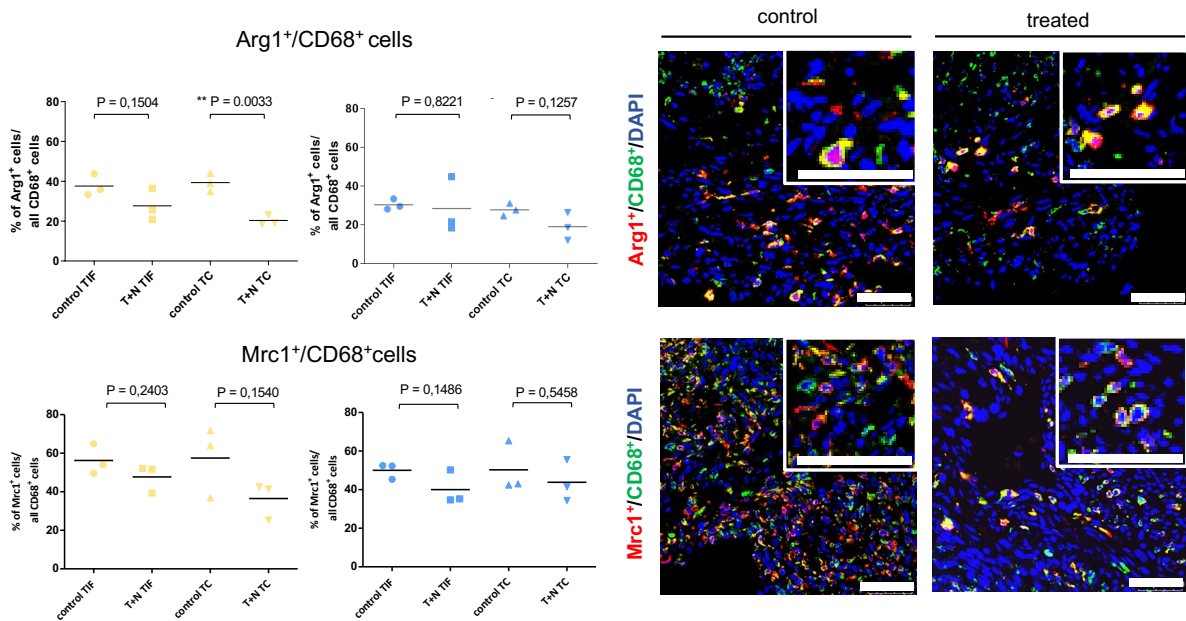
b

M1-like Macrophages



c

M2-like Macrophages



TIF = tumor invasive front
 TC = tumor core
 Control = non-treated
 N+T = combinational treatment (Nintedanib+Trametinib)

Figure 10 Combinatorial treatment with Trametinib and Nintedanib enhances infiltration of M1-like macrophages into the tumor tissue

a, Quantification of macrophage pan lineage marker CD68 from immunofluorescent staining representative depicted right. Phalloidin used to stain actin filaments and show shape of tumor cells. Counting results showing higher TAM infiltration in tumors derived from mesenchymal cell line (consistent to counting results of orthotopically implanted PDAC depicted in F6A). Corresponding to flow cytometry analysis (F8B), no numerous difference between untreated and double-treated PDAC cohorts could be detected. P-value of performed t-test above quantification results.

b, Quantification of M1-like macrophage polarization markers. Counting CD80⁺/CD68⁺- and iNOS⁺/CD68⁺-cells (double stained). (left) Quantification results indicating an increased M1-like TAM infiltration and

c, A decrease of M2-like TAM infiltration into the treatment –samples compared to the controls. Quantifying M2-like macrophage polarization markers. Counting Arg1⁺/CD68⁻ and Mrc1⁺/CD68⁺-cells (double stained). (right) Representative pictures for M1- and M2-polarized macrophages of immunofluorescent imaging.

Counting results being consistent between classical and mesenchymal tumor samples.

Note: At least 3 tumors and 5 fields of view per subtype and TAM group were counted. P-values of performed t-tests are shown above quantification results left. Scale 25 μm , respectively 50 μm in the top right corner.

Altogether, our results suggested diverse changes in the immune compartment of PDAC upon the combinatorial treatment with Trametinib and Nintedanib, including an increase in pro-inflammatory M1 features of TAMs.

4.4. Conclusion

To achieve more successful therapeutical strategies targeting PDAC getting a deeper comprehension of the TME is decisive. In this study, we performed a systematic characterization of the immune cell compartment focusing on the myeloid cell population, thereby in particular elucidating the immunosuppressive protumoral features of TAMs. To depict all relevant aspects, we studied the monocyte and macrophage cohort in the classical and mesenchymal PDAC subtypes, critical for the prognosis and immune cell composition of PDAC, and in an even more complex model of endogenous *Kras*^{G12D}-driven PDAC.

The tumor samples exhibited a great inter- and intratumoral heterogeneity of the myeloid cell compartment with a considerable higher infiltration in the more aggressive mesenchymal subtype, suggesting an intense crosstalk between tumor and immune cells. Moreover, we revealed the complex signatures of distinct TAM subclusters.

Taken together, this study enhanced the understanding of macrophage subpopulations and their immunosuppressive profiles emphasizing the role of TAMs as potential targets for the improvement of PDAC therapy. Thus, pointing out promising markers for further investigation especially moving the complement factors and *Spp1* in the center of interest.

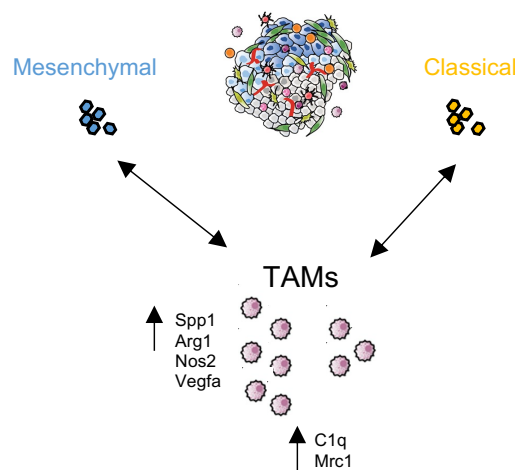


Figure 11 Summary of key immunosuppressive TAM -features found by scRNA-seq of distinct molecular PDAC subtypes

TME in mesenchymal PDAC samples (left) showing higher macrophage infiltration and upregulation of *Spp1* accompanied by hypoxic signatures on TAMs compared to classical ones (right). Both molecular subtypes (mesenchymal and classical) present an increase of complement factors on TAMs.

Taken together suggesting a crosstalk between PDAC cells and TAMs in the TME.

Illustration of the graph by courtesy of Chiara Falcomatà.

5. DISCUSSION

PDAC is a lethal disease and despite great efforts done in research still a leading cause of cancer-related death (Grossberg et al., 2020; Siegel et al., 2023). It contains a unique stromal compartment being highly desmoplastic and a tremendous range of immune cells. Together, they are shaping a complex TME with great inter- and intratumoral heterogeneity (Erkan et al., 2012; Foster et al., 2018; Ho et al., 2020; Hwang et al., 2022). An intense crosstalk between cancer and immune cells helps PDAC to overcome anticancer immunity and even allows tumor cells to hijack immune cell capacities and enhance their tumor promoting properties. In this regard, especially the myeloid cell compartment, in particular TAMs with their potential immunosuppressive and protumoral features, moved into the center of interest (Ansari et al., 2017; Bärthel et al., 2023; Condeelis & Pollard, 2006; Cox et al., 2021; Falcomatà et al., 2023; Pollard, 2004; Swietlik et al., 2023).

Moreover, it was shown that genetic alterations, as oncogenic *KRAS*, can influence the immune composition in the TME (Mueller et al., 2018; Wellenstein & de Visser, 2018).

In addition, studies of Collisson, Moffit and Bailey revealed distinct molecular subtypes of PDAC (Bailey et al., 2016; Collisson et al., 2011; Moffitt et al., 2015). Taken together, the classical and the mesenchymal subtype, which turned out to be the two major subgroups of PDAC, were shown to be able to influence the immune cell infiltration into the TME (Raghavan et al., 2021; Tu et al., 2021).

To date, there is a lack of clear characterization of myeloid cells, specifically TAM subpopulations and their immunosuppressive signatures, especially when taking in account the association with *KRAS* as oncogenic driver mutation as well as the impact of distinct PDAC subtypes on the TME composition.

To address the purpose of getting a deeper understanding of the TME in PDAC, we implemented a multimodal approach comprising immunofluorescent imaging by Confocal Microscopy, to depict TAM phenotypes and their spatial distribution, and the high-resolution methods flow cytometry and scRNA-seq analysis, using a GEMM and an orthotopic implantation model of PDAC.

Thereby, this study underlines TAMs and their corresponding immunosuppressive markers as potential targets for future therapy.

5.1. Impacts on TAM phenotype in PDAC

Hanahan and Weinberg proclaimed a next generation of cancer hallmarks. Thus, labelling tumor promoting inflammation as a critical aspect, contributing to multiple hallmark capabilities of tumor cells and respecting the central role of the TME, including its broad range of immune cells, in sustaining tumor growth (Hanahan & Weinberg, 2011). In addition, Mantovani et al. annotated the importance of considering oncogenic-activity as “intrinsic pathway”, as well as cellular and humoral immunity as “extrinsic pathway”, when studying cancer (Mantovani, Allavena, Sica, & Balkwill, 2008). Thereby, supporting our aim to characterize the immune cohort of the TME in PDAC in all its complexity.

5.1.1. Genetic alterations

GEMMs are potent models replicate the genetic landscape of the human disease in its great complexity. Distinct genetic alterations were shown to inter alia direct the innate immunity, thereby creating a relationship between the geno- and the phenotype in cancer (Blagih et al., 2020; Wellenstein & de Visser, 2018). Oncogenic *KRAS* as a

driver mutation of PDAC highly impacts the TME composition. It was found to influence the expression of cytokine-receptors on tumor cells and beyond that, to affect immunosuppressive immune cells to infiltrate the TME by regulating cytokine secretion (Dey et al., 2020). Bayne and Pylayeva-Gupta showed, *KRAS*-driven PDAC mediates immune evasion of cancer cells by secreting *GM-CSF*, leading to the infiltration of *CD11b⁺Gr1⁺* myeloid cells into the TME. By this, disrupting Ag-specific T-cell response and promoting an increase of other immunosuppressive cells as Tregs (Bayne et al., 2012; Pylayeva-Gupta et al., 2012). Moreover, *in vitro* experiments showed *Ras* oncogenes support PanIN progression by stimulating myeloid cells to secrete the cytokine IL-6 (Bayne et al., 2012; Wellenstein & de Visser, 2018). Compatible to these findings the characterization of the immune cell infiltration in our endogenous *Kras^{G12D}*-driven PDAC model by flow cytometry elucidated macrophages and neutrophils as the biggest immune cell cohorts in the TME. Additionally, further analysis of the TAM population revealed a strong predominance of immunosuppressive M2-like features in our immunofluorescent imaging as well as in our scRNA-seq data analysis.

PDAC is a complex disease, mostly containing a mixture of the classical and the mesenchymal subtypes, thereby also advancing the heterogeneity of its TME (Grunwald et al., 2021; Han et al., 2021). On top of that, the amplification of oncogenic *KRAS* was shown to be associated with more aggressive mesenchymal signatures in PDAC (Mueller et al., 2018; Raghavan et al., 2021). Maybe, these insights can in part explain the intertumoral heterogeneity, meaning the TAM high and TAM low PDAC samples, we found in our flow cytometry and immunofluorescent imaging analysis, as well as the intratumoral heterogeneity of the found monocyte and macrophage subclusters in the scRNA-seq analysis of our endogenous PDAC cohort being much bigger compared to the well-defined molecular subtypes (classical and mesenchymal) in our orthotopic implantation model.

5.1.2. Transcriptional subtypes

Distinct molecular subtypes of PDAC, previously described by Collisson, Moffitt and Bailey, (Bailey et al., 2016; Collisson et al., 2011; Moffitt et al., 2015) are suggested to harbor specific differences of their TME. Hwang et al. even recently identified a “treatment-enriched” PDAC subtype, accompanied with a high amount of CD8⁺-T-cells, which is increased upon chemo- and radiotherapy and associated with a poor prognosis (Hwang et al., 2022). Moreover, there is rising evidence of the intense crosstalk between distinct tumor and immune cells influencing the immune landscape of PDAC, partially in a subtype-specific manner (Bärthel et al., 2023; Wellenstein & de Visser, 2018). Thus, we aimed to characterize the immune composition in an orthotopic implantation model of PDAC, using in our lab previously generated well-characterized and *in vivo* tested cell-lines displaying the strongest classical or mesenchymal features (Falcomatà et al., 2022; Mueller et al., 2018). The more aggressive mesenchymal subtype, shown to be associated with a poor prognosis (Maurer et al., 2019), was found to actively contribute to the EMT-process by attracting *TNF α* -secreting macrophages through the release of the chemo-attractive molecule *Ccl2* (Tu et al., 2021). By that, matching with our findings of the mesenchymal subtype, compared to the classical one, being more affluent in myeloid cells, particularly in TAMs displaying a predominance of the immunosuppressive M2-polarization.

Furthermore, the found association of the mesenchymal cancer cells with a subpopulation of *C1qc^{high}* macrophages (Raghavan et al., 2021) underlines the subtype-specific impact on immune cells in PDAC and the necessity of its clear characterization.

5.2. TAM characteristics

PDAC contains a complex TME with a variety of immune cells. Among them especially TAMs are a highly versatile cohort, able to adopt distinct polarization states. Being able to address this heterogeneous group including its subpopulations it is crucial to use, besides commonly established technologies as immunofluorescent imaging and cell-sorting by flow cytometry, advanced versions of high-resolution methods. From these, scRNA-seq analysis is a valuable tool to achieve in depth characterization of immune cell populations in the TME apart from previously set marker genes (Falcomatà et al., 2023; Giladi & Amit, 2018; Han et al., 2021; Sun et al., 2021).

5.2.1. Immunosuppressive pathways

The scRNA-seq analysis of our endogenous as well as of our orthotopic implanted PDAC cohort elucidated the presence of a $C1q^{high}$ TAM subpopulation. In addition, these complement-high subclusters displayed elevated expression of *Mrc1* and *ApoE* as signatures of alternatively activated macrophages and highly exhibited HLA-associated genes. Moreover, preferentially displaying TR features. Taken together, the above-described signatures of these subclusters are consistent with $C1q^+$ TAM subpopulations described by Kemp and Revel (Kemp et al., 2021; Revel et al., 2022). TAMs with raised complement markers were shown to be associated with a M2-polarization and suggested to promote cancer progression by disturbing effective immune surveillance inter alia by mediating T-cell exhaustion by upregulating the expression of *PD-L1/2* (Roumenina et al., 2019) or through the *CXCL10-CXCR3*-axis, leading to an increase of Tregs (Revel et al., 2022). Furthermore, tumor cells can hijack complement factors produced by TAMs to activate the classical complement pathway (Roumenina et al., 2019) and help cancer cells to circumvent complement-mediated cell death by inducing a deficiency of the terminal complement pathway (Revel et al., 2022). For instance, Zhang et al. showed TAMs are leading to an increase in *Cd59* through an *IL6-R/STAT3* pathway, thereby inhibiting the formation of a membrane attack complex (R. Zhang et al., 2019). Beyond that, *PTX3* was demonstrated to regulate the complement cascade on tumor cells, additionally its deficiency in mice led to complement activation and secretion of *Ccl2*, resulting in the attraction of protumoral macrophages into the TME (Bonavita et al., 2015).

Besides the described interaction with tumor cells, $C1q^+$ macrophages were also shown to cooperate with other immune cells as a subpopulation of *C1q*-producing CAFs, shaping TAMs towards an immunosuppressive phenotype. Moreover, the found co-expression of HLA-associated genes on $C1q^+$ TAMs, also present in our complement-high macrophage subpopulations, were suggested to sustain those immune-immune crosstalks (Revel et al., 2022).

Another characteristic of TAM and monocyte subpopulations found in our both PDAC cohorts (endogenous and orthotopic implanted) is the elevated expression of *Spp1*. Concordant with our findings Wei et al. described an increase of *Spp1* on TAMs compared to macrophages in normal tissue, proposing a TME-related expression (Wei et al., 2021). Strikingly, our $Spp1^{high}$ TAM and monocyte subclusters were highly correlated to markers associated with hypoxia, as the potent angiogenic factor *Vegfa*. Moreover, we detected elevated levels of *iNOS* and *Arg1*, matching to the dysregulated metabolism in hypoxic tumor areas described by Doedens and Colegio (Colegio et al., 2014; Doedens et al., 2010). *Arg1* and *iNOS* are both competitive L-Arginine consuming enzymes, thereby contributing to macrophage-driven T-cell exhaustion. Of them, especially the immunosuppressive marker *Arg1* is increased due to the presence of *HIF1 α* (Doedens et al., 2010) and lactic acids as a byproduct of glycolysis (Colegio

et al., 2014). Moreover, *Arg1* was shown to dampen the formation of the T-cell receptor's *CD3 ζ* chain by depleting L-Arginine from the TME and additionally supporting a rapid cancer cell proliferation by producing polyamines, need for an active cell cycle program (Rodriguez et al., 2004). Altogether, hypoxia in the TME was shown to increase the number of *Spp1*⁺ TAMs, which in turn promote tumor progression *inter alia* by secreting MMPs, thereby contributing to ECM-remodeling and EMT (Bärthel et al., 2023; Wei et al., 2021).

Thus, high expression of *C1q* as well as *Spp1* on TAMs takes a central role in fostering tumor growth and metastasis.

Comparable as described above for *C1q*⁺ TAMs, there is moreover an immune-immune crosstalk of a *FAP*⁺ CAF subpopulation with TAMs sustaining the differentiation of a *Spp1*⁺ TAM subcluster (Qi et al., 2022).

In addition, we detected a distinction concerning the composition of our monocyte/macrophage cohort between the molecular subtypes (classical and mesenchymal) of our orthotopic implantation model. Of them, the more aggressive mesenchymal subtype preferentially contributed to the *Spp1*^{high} Macrophage cluster, which eponymous marker was shown to promote EMT (Wei et al., 2021). Whereas, both subtypes, with a slight predominance of the classical PDAC samples, constituted the TR *C1q*^{high} Macrophage cluster.

5.2.2. Involvement in therapy response

Therapeutic approaches do not only address tumor cells but can also lead to a modulation of the TME. Upon our recently published combinatorial treatment strategy, combining the kinase-inhibitors Trametinib and Nintedanib, we detected an increase of effector T-cells *in vivo*, which led to an enhanced efficacy of *PD-L1* blockade in the mesenchymal PDAC subtype. Moreover, we found a rise of pro-inflammatory features on TAMs analyzed by immunofluorescent imaging (Falcomatà et al., 2022). Correspondingly, Steele et al. described immune checkpoint signals being higher in the mesenchymal compared to the classical subtype. Furthermore, they found myeloid cells, particularly alternatively activated macrophages, are an essential source of immune checkpoint ligands in pancreatic cancer (Steele et al., 2020). Besides that, macrophages were shown to be involved in resistance-mechanism towards ICB-therapy accompanied by a unique immunosuppressive cytokine-milieu shaping the T-cell cohort in the TME (Aslan et al., 2020).

Thus, TAMs play a crucial role in successful therapy response by strongly affecting the TME composition upon treatment, being in turn influenced by distinct signals of the molecular PDAC subtypes.

5.3. Outlook

This study presents a systematic characterization of the immune cell compartment in PDAC, focusing on the monocyte and macrophage populations. Therefore, using an endogenous *Kras*^{G12D}-driven and an orthotopic implantation model to discover the impact of genetic alterations and transcriptional subtypes on the TME. Our results improve the understanding of the myeloid cell biology, in particular elucidating the key immunosuppressive features of TAMs and highlights them as potential targets for improving PDAC therapy.

Prospective, we aim to get an even deeper comprehension of how distinct TAM subsets and their highly expressed gene signatures influence PDAC development and if their abundance correlates with tumor progression, clinical outcome and therapy response. Moreover, we want to detect how the distinct molecular PDAC subtypes in detail mediate myeloid cell recruitment and shape their phenotype, especially which tumor-immune and immune-immune signaling axis are involved. In addition, we want to compare our data to those evolving from human data sets.

This far-reaching analysis will result in depth understanding of distinct TAM subsets and their immunosuppressive pathways and confidently will impact future therapeutic approaches of PDAC.

6. References

- Ambrogio, C., Köhler, J., Zhou, Z. W., Wang, H., Paranal, R., Li, J., . . . Jänne, P. A. (2018). KRAS Dimerization Impacts MEK Inhibitor Sensitivity and Oncogenic Activity of Mutant KRAS. *Cell*, *172*(4), 857-868.e815. doi:10.1016/j.cell.2017.12.020
- Ansari, D., Carvajo, M., Bauden, M., & Andersson, R. (2017). Pancreatic cancer stroma: controversies and current insights. *Scand J Gastroenterol*, *52*(6-7), 641-646. doi:10.1080/00365521.2017.1293726
- Arlauckas, S. P., Garren, S. B., Garris, C. S., Kohler, R. H., Oh, J., Pittet, M. J., & Weissleder, R. (2018). Arg1 expression defines immunosuppressive subsets of tumor-associated macrophages. *Theranostics*, *8*(21), 5842-5854. doi:10.7150/thno.26888
- Aslan, K., Turco, V., Blobner, J., Sonner, J. K., Liuzzi, A. R., Núñez, N. G., . . . Platten, M. (2020). Heterogeneity of response to immune checkpoint blockade in hypermutated experimental gliomas. *Nat Commun*, *11*(1), 931. doi:10.1038/s41467-020-14642-0
- Aung, K. L., Fischer, S. E., Denroche, R. E., Jang, G. H., Dodd, A., Creighton, S., . . . Knox, J. J. (2018). Genomics-Driven Precision Medicine for Advanced Pancreatic Cancer: Early Results from the COMPASS Trial. *Clin Cancer Res*, *24*(6), 1344-1354. doi:10.1158/1078-0432.Ccr-17-2994
- Bailey, P., Chang, D. K., Nones, K., Johns, A. L., Patch, A. M., Gingras, M. C., . . . Grimmond, S. M. (2016). Genomic analyses identify molecular subtypes of pancreatic cancer. *Nature*, *531*(7592), 47-52. doi:10.1038/nature16965
- Bärthel, S., Falcomatà, C., Rad, R., Theis, F. J., & Saur, D. (2023). Single-cell profiling to explore pancreatic cancer heterogeneity, plasticity and response to therapy. *Nat Cancer*, *4*(4), 454-467. doi:10.1038/s43018-023-00526-x
- Bayne, L. J., Beatty, G. L., Jhala, N., Clark, C. E., Rhim, A. D., Stanger, B. Z., & Vonderheide, R. H. (2012). Tumor-derived granulocyte-macrophage colony-stimulating factor regulates myeloid inflammation and T cell immunity in pancreatic cancer. *Cancer Cell*, *21*(6), 822-835. doi:10.1016/j.ccr.2012.04.025
- Bear, A. S., Vonderheide, R. H., & O'Hara, M. H. (2020). Challenges and Opportunities for Pancreatic Cancer Immunotherapy. *Cancer Cell*, *38*(6), 788-802. doi:10.1016/j.ccell.2020.08.004
- Becht, E., McInnes, L., Healy, J., Dutertre, C. A., Kwok, I. W. H., Ng, L. G., . . . Newell, E. W. (2018). Dimensionality reduction for visualizing single-cell data using UMAP. *Nat Biotechnol*. doi:10.1038/nbt.4314
- Bergman, A. M., Pinedo, H. M., & Peters, G. J. (2002). Determinants of resistance to 2',2'-difluorodeoxycytidine (gemcitabine). *Drug Resist Updat*, *5*(1), 19-33. doi:10.1016/s1368-7646(02)00002-x
- Bertani, F. R., Mozetic, P., Fioramonti, M., Iuliani, M., Ribelli, G., Pantano, F., . . . Rainer, A. (2017). Classification of M1/M2-polarized human macrophages by label-free hyperspectral reflectance confocal microscopy and multivariate analysis. *Sci Rep*, *7*(1), 8965. doi:10.1038/s41598-017-08121-8
- Binnewies, M., Roberts, E. W., Kersten, K., Chan, V., Fearon, D. F., Merad, M., . . . Krummel, M. F. (2018). Understanding the tumor immune microenvironment (TIME) for effective therapy. *Nat Med*, *24*(5), 541-550. doi:10.1038/s41591-018-0014-x
- Blagih, J., Zani, F., Chakravarty, P., Hennequart, M., Pilley, S., Hobor, S., . . . Vousden, K. H. (2020). Cancer-Specific Loss of p53 Leads to a Modulation of Myeloid and T Cell Responses. *Cell Rep*, *30*(2), 481-496.e486. doi:10.1016/j.celrep.2019.12.028
- Bonavita, E., Gentile, S., Rubino, M., Maina, V., Papait, R., Kunderfranco, P., . . . Mantovani, A. (2015). PTX3 is an extrinsic oncosuppressor regulating complement-dependent inflammation in cancer. *Cell*, *160*(4), 700-714. doi:10.1016/j.cell.2015.01.004
- Bosetti, C., Lucenteforte, E., Silverman, D. T., Petersen, G., Bracci, P. M., Ji, B. T., . . . La Vecchia, C. (2012). Cigarette smoking and pancreatic cancer: an analysis from the International Pancreatic Cancer Case-Control Consortium (Panc4). *Ann Oncol*, *23*(7), 1880-1888. doi:10.1093/annonc/mdr541

- Boutillier, A. J., & Elswa, S. F. (2021). Macrophage Polarization States in the Tumor Microenvironment. *Int J Mol Sci*, 22(13). doi:10.3390/ijms22136995
- Brennan, M. F., Kattan, M. W., Klimstra, D., & Conlon, K. (2004). Prognostic nomogram for patients undergoing resection for adenocarcinoma of the pancreas. *Ann Surg*, 240(2), 293-298. doi:10.1097/01.sla.0000133125.85489.07
- Calderon, B., Carrero, J. A., Ferris, S. T., Sojka, D. K., Moore, L., Epelman, S., . . . Unanue, E. R. (2015). The pancreas anatomy conditions the origin and properties of resident macrophages. *J Exp Med*, 212(10), 1497-1512. doi:10.1084/jem.20150496
- Carioli, G., Malvezzi, M., Bertuccio, P., Boffetta, P., Levi, F., La Vecchia, C., & Negri, E. (2021). European cancer mortality predictions for the year 2021 with focus on pancreatic and female lung cancer. *Ann Oncol*, 32(4), 478-487. doi:10.1016/j.annonc.2021.01.006
- Coelho, M. A., de Carné Trécesson, S., Rana, S., Zecchin, D., Moore, C., Molina-Arcas, M., . . . Downward, J. (2017). Oncogenic RAS Signaling Promotes Tumor Immuno-resistance by Stabilizing PD-L1 mRNA. *Immunity*, 47(6), 1083-1099.e1086. doi:10.1016/j.immuni.2017.11.016
- Colegio, O. R., Chu, N. Q., Szabo, A. L., Chu, T., Rhebergen, A. M., Jairam, V., . . . Medzhitov, R. (2014). Functional polarization of tumour-associated macrophages by tumour-derived lactic acid. *Nature*, 513(7519), 559-563. doi:10.1038/nature13490
- Collisson, E. A., Sadanandam, A., Olson, P., Gibb, W. J., Truitt, M., Gu, S., . . . Gray, J. W. (2011). Subtypes of pancreatic ductal adenocarcinoma and their differing responses to therapy. *Nat Med*, 17(4), 500-503. doi:10.1038/nm.2344
- Collisson, E. A., Trejo, C. L., Silva, J. M., Gu, S., Korkola, J. E., Heiser, L. M., . . . McMahon, M. (2012). A central role for RAF→MEK→ERK signaling in the genesis of pancreatic ductal adenocarcinoma. *Cancer Discov*, 2(8), 685-693. doi:10.1158/2159-8290.Cd-11-0347
- Condeelis, J., & Pollard, J. W. (2006). Macrophages: obligate partners for tumor cell migration, invasion, and metastasis. *Cell*, 124(2), 263-266. doi:10.1016/j.cell.2006.01.007
- Cortesi, M., Zanoni, M., Pirini, F., Tumedei, M. M., Ravaioli, S., Rapposelli, I. G., . . . Bravaccini, S. (2021). Pancreatic Cancer and Cellular Senescence: Tumor Microenvironment under the Spotlight. *Int J Mol Sci*, 23(1). doi:10.3390/ijms23010254
- Cox, N., Pokrovskii, M., Vicario, R., & Geissmann, F. (2021). Origins, Biology, and Diseases of Tissue Macrophages. *Annu Rev Immunol*, 39, 313-344. doi:10.1146/annurev-immunol-093019-111748
- Daley, D., Mani, V. R., Mohan, N., Akkad, N., Ochi, A., Heindel, D. W., . . . Miller, G. (2017). Dectin 1 activation on macrophages by galectin 9 promotes pancreatic carcinoma and peritumoral immune tolerance. *Nat Med*, 23(5), 556-567. doi:10.1038/nm.4314
- Daley, D., Mani, V. R., Mohan, N., Akkad, N., Pandian, G., Savadkar, S., . . . Miller, G. (2017). NLRP3 signaling drives macrophage-induced adaptive immune suppression in pancreatic carcinoma. *J Exp Med*, 214(6), 1711-1724. doi:10.1084/jem.20161707
- DeNardo, D. G., Barreto, J. B., Andreu, P., Vasquez, L., Tawfik, D., Kolhatkar, N., & Coussens, L. M. (2009). CD4(+) T cells regulate pulmonary metastasis of mammary carcinomas by enhancing protumor properties of macrophages. *Cancer Cell*, 16(2), 91-102. doi:10.1016/j.ccr.2009.06.018
- Deng, D., Patel, R., Chiang, C. Y., & Hou, P. (2022). Role of the Tumor Microenvironment in Regulating Pancreatic Cancer Therapy Resistance. *Cells*, 11(19). doi:10.3390/cells11192952
- Dey, P., Li, J., Zhang, J., Chaurasiya, S., Strom, A., Wang, H., . . . DePinho, R. A. (2020). Oncogenic KRAS-Driven Metabolic Reprogramming in Pancreatic Cancer Cells Utilizes Cytokines from the Tumor Microenvironment. *Cancer Discov*, 10(4), 608-625. doi:10.1158/2159-8290.Cd-19-0297
- Doedens, A. L., Stockmann, C., Rubinstein, M. P., Liao, D., Zhang, N., DeNardo, D. G., . . . Johnson, R. S. (2010). Macrophage expression of hypoxia-inducible factor-1 alpha suppresses T-cell function and promotes tumor progression. *Cancer Res*, 70(19), 7465-7475. doi:10.1158/0008-5472.Can-10-1439

- Dominguez, C. X., Müller, S., Keerthivasan, S., Koeppen, H., Hung, J., Gierke, S., . . . Turley, S. J. (2020). Single-Cell RNA Sequencing Reveals Stromal Evolution into LRRRC15(+) Myofibroblasts as a Determinant of Patient Response to Cancer Immunotherapy. *Cancer Discov*, *10*(2), 232-253. doi:10.1158/2159-8290.Cd-19-0644
- Elyada, E., Bolisetty, M., Laise, P., Flynn, W. F., Courtois, E. T., Burkhart, R. A., . . . Tuveson, D. A. (2019). Cross-Species Single-Cell Analysis of Pancreatic Ductal Adenocarcinoma Reveals Antigen-Presenting Cancer-Associated Fibroblasts. *Cancer Discov*, *9*(8), 1102-1123. doi:10.1158/2159-8290.Cd-19-0094
- Erkan, M., Hausmann, S., Michalski, C. W., Fingerle, A. A., Dobritz, M., Kleeff, J., & Friess, H. (2012). The role of stroma in pancreatic cancer: diagnostic and therapeutic implications. *Nat Rev Gastroenterol Hepatol*, *9*(8), 454-467. doi:10.1038/nrgastro.2012.115
- Falcomatà, C., Bärthel, S., Schneider, G., Rad, R., Schmidt-Suprian, M., & Saur, D. (2023). Context-Specific Determinants of the Immunosuppressive Tumor Microenvironment in Pancreatic Cancer. *Cancer Discov*, *13*(2), 278-297. doi:10.1158/2159-8290.Cd-22-0876
- Falcomatà, C., Bärthel, S., Schneider, G., Saur, D., & Veltkamp, C. (2019). Deciphering the universe of genetic context-dependencies using mouse models of cancer. *Curr Opin Genet Dev*, *54*, 97-104. doi:10.1016/j.gde.2019.04.002
- Falcomatà, C., Bärthel, S., Widholz, S. A., Schneeweis, C., Montero, J. J., Toska, A., . . . Saur, D. (2022). Selective multi-kinase inhibition sensitizes mesenchymal pancreatic cancer to immune checkpoint blockade by remodeling the tumor microenvironment. *Nat Cancer*, *3*(3), 318-336. doi:10.1038/s43018-021-00326-1
- Fan, J. Q., Wang, M. F., Chen, H. L., Shang, D., Das, J. K., & Song, J. (2020). Current advances and outlooks in immunotherapy for pancreatic ductal adenocarcinoma. *Mol Cancer*, *19*(1), 32. doi:10.1186/s12943-020-01151-3
- Feldmann, G., Beaty, R., Hruban, R. H., & Maitra, A. (2007). Molecular genetics of pancreatic intraepithelial neoplasia. *J Hepatobiliary Pancreat Surg*, *14*(3), 224-232. doi:10.1007/s00534-006-1166-5
- Foster, D. S., Jones, R. E., Ransom, R. C., Longaker, M. T., & Norton, J. A. (2018). The evolving relationship of wound healing and tumor stroma. *JCI Insight*, *3*(18). doi:10.1172/jci.insight.99911
- Gibbs, J. B., Sigal, I. S., Poe, M., & Scolnick, E. M. (1984). Intrinsic GTPase activity distinguishes normal and oncogenic ras p21 molecules. *Proc Natl Acad Sci U S A*, *81*(18), 5704-5708. doi:10.1073/pnas.81.18.5704
- Giladi, A., & Amit, I. (2018). Single-Cell Genomics: A Stepping Stone for Future Immunology Discoveries. *Cell*, *172*(1-2), 14-21. doi:10.1016/j.cell.2017.11.011
- Gomez Perdiguero, E., & Geissmann, F. (2014). Cancer immunology. Identifying the infiltrators. *Science*, *344*(6186), 801-802. doi:10.1126/science.1255117
- Gomez Perdiguero, E., Klapproth, K., Schulz, C., Busch, K., Azzoni, E., Crozet, L., . . . Rodewald, H. R. (2015). Tissue-resident macrophages originate from yolk-sac-derived erythro-myeloid progenitors. *Nature*, *518*(7540), 547-551. doi:10.1038/nature13989
- Gordon, S., Plüddemann, A., & Martinez Estrada, F. (2014). Macrophage heterogeneity in tissues: phenotypic diversity and functions. *Immunol Rev*, *262*(1), 36-55. doi:10.1111/imr.12223
- Grossberg, A. J., Chu, L. C., Deig, C. R., Fishman, E. K., Hwang, W. L., Maitra, A., . . . Thomas, C. R., Jr. (2020). Multidisciplinary standards of care and recent progress in pancreatic ductal adenocarcinoma. *CA Cancer J Clin*, *70*(5), 375-403. doi:10.3322/caac.21626
- Grunwald, B. T., Devisme, A., Andrieux, G., Vyas, F., Aliar, K., McCloskey, C. W., . . . Khokha, R. (2021). Spatially confined sub-tumor microenvironments in pancreatic cancer. *Cell*, *184*(22), 5577-5592 e5518. doi:10.1016/j.cell.2021.09.022
- Han, J., DePinho, R. A., & Maitra, A. (2021). Single-cell RNA sequencing in pancreatic cancer. *Nat Rev Gastroenterol Hepatol*, *18*(7), 451-452. doi:10.1038/s41575-021-00471-z
- Hanahan, D., & Weinberg, R. A. (2011). Hallmarks of cancer: the next generation. *Cell*, *144*(5), 646-674. doi:10.1016/j.cell.2011.02.013

- Hingorani, S. R., Petricoin, E. F., Maitra, A., Rajapakse, V., King, C., Jacobetz, M. A., . . . Tuveson, D. A. (2003). Preinvasive and invasive ductal pancreatic cancer and its early detection in the mouse. *Cancer Cell*, 4(6), 437-450. doi:10.1016/s1535-6108(03)00309-x
- Ho, W. J., Jaffee, E. M., & Zheng, L. (2020). The tumour microenvironment in pancreatic cancer - clinical challenges and opportunities. *Nat Rev Clin Oncol*, 17(9), 527-540. doi:10.1038/s41571-020-0363-5
- Hou, P., & Wang, Y. A. (2022). Conquering oncogenic KRAS and its bypass mechanisms. *Theranostics*, 12(13), 5691-5709. doi:10.7150/thno.71260
- Hughes, R., Qian, B. Z., Rowan, C., Muthana, M., Keklikoglou, I., Olson, O. C., . . . Lewis, C. E. (2015). Perivascular M2 Macrophages Stimulate Tumor Relapse after Chemotherapy. *Cancer Res*, 75(17), 3479-3491. doi:10.1158/0008-5472.Can-14-3587
- Hwang, W. L., Jagadeesh, K. A., Guo, J. A., Hoffman, H. I., Yadollahpour, P., Reeves, J. W., . . . Regev, A. (2022). Single-nucleus and spatial transcriptome profiling of pancreatic cancer identifies multicellular dynamics associated with neoadjuvant treatment. *Nat Genet*, 54(8), 1178-1191. doi:10.1038/s41588-022-01134-8
- Ilic, M., & Ilic, I. (2016). Epidemiology of pancreatic cancer. *World J Gastroenterol*, 22(44), 9694-9705. doi:10.3748/wjg.v22.i44.9694
- Integrated Genomic Characterization of Pancreatic Ductal Adenocarcinoma. (2017). *Cancer Cell*, 32(2), 185-203.e113. doi:10.1016/j.ccell.2017.07.007
- Jackson, E. L., Willis, N., Mercer, K., Bronson, R. T., Crowley, D., Montoya, R., . . . Tuveson, D. A. (2001). Analysis of lung tumor initiation and progression using conditional expression of oncogenic K-ras. *Genes Dev*, 15(24), 3243-3248. doi:10.1101/gad.943001
- Jaynes, J. M., Sable, R., Ronzetti, M., Bautista, W., Knotts, Z., Abisoye-Ogunniyan, A., . . . Rudloff, U. (2020). Mannose receptor (CD206) activation in tumor-associated macrophages enhances adaptive and innate antitumor immune responses. *Sci Transl Med*, 12(530). doi:10.1126/scitranslmed.aax6337
- Kalbasi, A., Komar, C., Tooker, G. M., Liu, M., Lee, J. W., Gladney, W. L., . . . Beatty, G. L. (2017). Tumor-Derived CCL2 Mediates Resistance to Radiotherapy in Pancreatic Ductal Adenocarcinoma. *Clin Cancer Res*, 23(1), 137-148. doi:10.1158/1078-0432.Ccr-16-0870
- Katzenelenbogen, Y., Sheban, F., Yalin, A., Yofe, I., Svetlichnyy, D., Jaitin, D. A., . . . Amit, I. (2020). Coupled scRNA-Seq and Intracellular Protein Activity Reveal an Immunosuppressive Role of TREM2 in Cancer. *Cell*, 182(4), 872-885.e819. doi:10.1016/j.cell.2020.06.032
- Kemp, S. B., Steele, N. G., Carpenter, E. S., Donahue, K. L., Bushnell, G. G., Morris, A. H., . . . Pasca di Magliano, M. (2021). Pancreatic cancer is marked by complement-high blood monocytes and tumor-associated macrophages. *Life Sci Alliance*, 4(6). doi:10.26508/lsa.202000935
- Khorana, A. A., Mangu, P. B., Berlin, J., Engebretson, A., Hong, T. S., Maitra, A., . . . Katz, M. H. G. (2017). Potentially Curable Pancreatic Cancer: American Society of Clinical Oncology Clinical Practice Guideline Update. *J Clin Oncol*, 35(20), 2324-2328. doi:10.1200/JCO.2017.72.4948
- Kim, J. E., Lee, K. T., Lee, J. K., Paik, S. W., Rhee, J. C., & Choi, K. W. (2004). Clinical usefulness of carbohydrate antigen 19-9 as a screening test for pancreatic cancer in an asymptomatic population. *J Gastroenterol Hepatol*, 19(2), 182-186. doi:10.1111/j.1440-1746.2004.03219.x
- Kitamura, T., Qian, B. Z., & Pollard, J. W. (2015). Immune cell promotion of metastasis. *Nat Rev Immunol*, 15(2), 73-86. doi:10.1038/nri3789
- Kuninaka, Y., Ishida, Y., Ishigami, A., Nosaka, M., Matsuki, J., Yasuda, H., . . . Kondo, T. (2022). Macrophage polarity and wound age determination. *Sci Rep*, 12(1), 20327. doi:10.1038/s41598-022-24577-9
- Larionova, I., Cherdyntseva, N., Liu, T., Patysheva, M., Rakina, M., & Kzhyshkowska, J. (2019). Interaction of tumor-associated macrophages and cancer chemotherapy. *Oncoimmunology*, 8(7), 1596004. doi:10.1080/2162402x.2019.1596004
- Lee, C., Jeong, H., Bae, Y., Shin, K., Kang, S., Kim, H., . . . Bae, H. (2019). Targeting of M2-like tumor-associated macrophages with a melittin-based pro-apoptotic peptide. *J Immunother Cancer*, 7(1), 147. doi:10.1186/s40425-019-0610-4

- Lee, S. R., Kim, H. O., Son, B. H., Yoo, C. H., & Shin, J. H. (2013). Prognostic factors associated with long-term survival and recurrence in pancreatic adenocarcinoma. *Hepatogastroenterology*, *60*(122), 358-362. doi:10.5754/hge12727
- Liu, C. Y., Xu, J. Y., Shi, X. Y., Huang, W., Ruan, T. Y., Xie, P., & Ding, J. L. (2013). M2-polarized tumor-associated macrophages promoted epithelial-mesenchymal transition in pancreatic cancer cells, partially through TLR4/IL-10 signaling pathway. *Lab Invest*, *93*(7), 844-854. doi:10.1038/labinvest.2013.69
- Mahon, O. R., Kelly, D. J., McCarthy, G. M., & Dunne, A. (2020). Osteoarthritis-associated basic calcium phosphate crystals alter immune cell metabolism and promote M1 macrophage polarization. *Osteoarthritis Cartilage*, *28*(5), 603-612. doi:10.1016/j.joca.2019.10.010
- Mallya, K., Gautam, S. K., Aithal, A., Batra, S. K., & Jain, M. (2021). Modeling pancreatic cancer in mice for experimental therapeutics. *Biochim Biophys Acta Rev Cancer*, *1876*(1), 188554. doi:10.1016/j.bbcan.2021.188554
- Manrai, M., Tilak, T., Dawra, S., Srivastava, S., & Singh, A. (2021). Current and emerging therapeutic strategies in pancreatic cancer: Challenges and opportunities. *World J Gastroenterol*, *27*(39), 6572-6589. doi:10.3748/wjg.v27.i39.6572
- Mantovani, A., Allavena, P., Sica, A., & Balkwill, F. (2008). Cancer-related inflammation. *Nature*, *454*(7203), 436-444. doi:10.1038/nature07205
- Mantovani, A., Sica, A., Sozzani, S., Allavena, P., Vecchi, A., & Locati, M. (2004). The chemokine system in diverse forms of macrophage activation and polarization. *Trends Immunol*, *25*(12), 677-686. doi:10.1016/j.it.2004.09.015
- Martinez, F. O., & Gordon, S. (2014). The M1 and M2 paradigm of macrophage activation: time for reassessment. *F1000Prime Rep*, *6*, 13. doi:10.12703/p6-13
- Maurer, C., Holmstrom, S. R., He, J., Laise, P., Su, T., Ahmed, A., . . . Olive, K. P. (2019). Experimental microdissection enables functional harmonisation of pancreatic cancer subtypes. *Gut*, *68*(6), 1034-1043. doi:10.1136/gutjnl-2018-317706
- McGrath, J. P., Capon, D. J., Goeddel, D. V., & Levinson, A. D. (1984). Comparative biochemical properties of normal and activated human ras p21 protein. *Nature*, *310*(5979), 644-649. doi:10.1038/310644a0
- Mechnikov, I. (1988). Immunity in infective diseases. By Ili'a Ilich Mechnikov, 1905. *Rev Infect Dis*, *10*(1), 223-227.
- Mills, C. D., Kincaid, K., Alt, J. M., Heilman, M. J., & Hill, A. M. (2000). M-1/M-2 macrophages and the Th1/Th2 paradigm. *J Immunol*, *164*(12), 6166-6173. doi:10.4049/jimmunol.164.12.6166
- Moffitt, R. A., Marayati, R., Flate, E. L., Volmar, K. E., Loeza, S. G., Hoadley, K. A., . . . Yeh, J. J. (2015). Virtual microdissection identifies distinct tumor- and stroma-specific subtypes of pancreatic ductal adenocarcinoma. *Nat Genet*, *47*(10), 1168-1178. doi:10.1038/ng.3398
- Mueller, S., Engleitner, T., Maresch, R., Zukowska, M., Lange, S., Kaltenbacher, T., . . . Rad, R. (2018). Evolutionary routes and KRAS dosage define pancreatic cancer phenotypes. *Nature*, *554*(7690), 62-68. doi:10.1038/nature25459
- Nakhai, H., Sel, S., Favor, J., Mendoza-Torres, L., Paulsen, F., Duncker, G. I., & Schmid, R. M. (2007). Ptf1a is essential for the differentiation of GABAergic and glycinergic amacrine cells and horizontal cells in the mouse retina. *Development*, *134*(6), 1151-1160. doi:10.1242/dev.02781
- Neesse, A., Michl, P., Frese, K. K., Feig, C., Cook, N., Jacobetz, M. A., . . . Tuveson, D. A. (2011). Stromal biology and therapy in pancreatic cancer. *Gut*, *60*(6), 861-868. doi:10.1136/gut.2010.226092
- Öhlund, D., Handly-Santana, A., Biffi, G., Elyada, E., Almeida, A. S., Ponz-Sarvise, M., . . . Tuveson, D. A. (2017). Distinct populations of inflammatory fibroblasts and myofibroblasts in pancreatic cancer. *J Exp Med*, *214*(3), 579-596. doi:10.1084/jem.20162024
- Orban, P. C., Chui, D., & Marth, J. D. (1992). Tissue- and site-specific DNA recombination in transgenic mice. *Proc Natl Acad Sci U S A*, *89*(15), 6861-6865. doi:10.1073/pnas.89.15.6861

- Polański, K., Young, M. D., Miao, Z., Meyer, K. B., Teichmann, S. A., & Park, J. E. (2020). BBKNN: fast batch alignment of single cell transcriptomes. *Bioinformatics*, *36*(3), 964-965. doi:10.1093/bioinformatics/btz625
- Pollard, J. W. (2004). Tumour-educated macrophages promote tumour progression and metastasis. *Nat Rev Cancer*, *4*(1), 71-78. doi:10.1038/nrc1256
- Puleo, F., Nicolle, R., Blum, Y., Cros, J., Marisa, L., Demetter, P., . . . Marechal, R. (2018). Stratification of Pancreatic Ductal Adenocarcinomas Based on Tumor and Microenvironment Features. *Gastroenterology*, *155*(6), 1999-2013 e1993. doi:10.1053/j.gastro.2018.08.033
- Pylayeva-Gupta, Y., Grabocka, E., & Bar-Sagi, D. (2011). RAS oncogenes: weaving a tumorigenic web. *Nat Rev Cancer*, *11*(11), 761-774. doi:10.1038/nrc3106
- Pylayeva-Gupta, Y., Lee, K. E., Hajdu, C. H., Miller, G., & Bar-Sagi, D. (2012). Oncogenic Kras-induced GM-CSF production promotes the development of pancreatic neoplasia. *Cancer Cell*, *21*(6), 836-847. doi:10.1016/j.ccr.2012.04.024
- Qi, J., Sun, H., Zhang, Y., Wang, Z., Xun, Z., Li, Z., . . . Su, B. (2022). Single-cell and spatial analysis reveal interaction of FAP(+) fibroblasts and SPP1(+) macrophages in colorectal cancer. *Nat Commun*, *13*(1), 1742. doi:10.1038/s41467-022-29366-6
- Qian, B. Z., Li, J., Zhang, H., Kitamura, T., Zhang, J., Campion, L. R., . . . Pollard, J. W. (2011). CCL2 recruits inflammatory monocytes to facilitate breast-tumour metastasis. *Nature*, *475*(7355), 222-225. doi:10.1038/nature10138
- Raghavan, S., Winter, P. S., Navia, A. W., Williams, H. L., DenAdel, A., Lowder, K. E., . . . Shalek, A. K. (2021). Microenvironment drives cell state, plasticity, and drug response in pancreatic cancer. *Cell*, *184*(25), 6119-6137.e6126. doi:10.1016/j.cell.2021.11.017
- Rahib, L., Smith, B. D., Aizenberg, R., Rosenzweig, A. B., Fleshman, J. M., & Matrisian, L. M. (2014). Projecting cancer incidence and deaths to 2030: the unexpected burden of thyroid, liver, and pancreas cancers in the United States. *Cancer Res*, *74*(11), 2913-2921. doi:10.1158/0008-5472.CAN-14-0155
- Raimondi, S., Lowenfels, A. B., Morselli-Labate, A. M., Maisonneuve, P., & Pezzilli, R. (2010). Pancreatic cancer in chronic pancreatitis; aetiology, incidence, and early detection. *Best Pract Res Clin Gastroenterol*, *24*(3), 349-358. doi:10.1016/j.bpg.2010.02.007
- Ren, B., Cui, M., Yang, G., Wang, H., Feng, M., You, L., & Zhao, Y. (2018). Tumor microenvironment participates in metastasis of pancreatic cancer. *Mol Cancer*, *17*(1), 108. doi:10.1186/s12943-018-0858-1
- Revel, M., Sautès-Fridman, C., Fridman, W. H., & Roumenina, L. T. (2022). C1q+ macrophages: passengers or drivers of cancer progression. *Trends Cancer*, *8*(7), 517-526. doi:10.1016/j.trecan.2022.02.006
- Ries, C. H., Cannarile, M. A., Hoves, S., Benz, J., Wartha, K., Runza, V., . . . Rüttinger, D. (2014). Targeting tumor-associated macrophages with anti-CSF-1R antibody reveals a strategy for cancer therapy. *Cancer Cell*, *25*(6), 846-859. doi:10.1016/j.ccr.2014.05.016
- Rodriguez, P. C., Quiceno, D. G., Zabaleta, J., Ortiz, B., Zea, A. H., Piazuelo, M. B., . . . Ochoa, A. C. (2004). Arginase I production in the tumor microenvironment by mature myeloid cells inhibits T-cell receptor expression and antigen-specific T-cell responses. *Cancer Res*, *64*(16), 5839-5849. doi:10.1158/0008-5472.Can-04-0465
- Roumenina, L. T., Daugan, M. V., Noé, R., Petitprez, F., Vano, Y. A., Sanchez-Salas, R., . . . Fridman, W. H. (2019). Tumor Cells Hijack Macrophage-Produced Complement C1q to Promote Tumor Growth. *Cancer Immunol Res*, *7*(7), 1091-1105. doi:10.1158/2326-6066.Cir-18-0891
- Ruffell, B., & Coussens, L. M. (2015). Macrophages and therapeutic resistance in cancer. *Cancer Cell*, *27*(4), 462-472. doi:10.1016/j.ccell.2015.02.015
- S, N. K., Wilson, G. W., Grant, R. C., Seto, M., O'Kane, G., Vajpeyi, R., . . . Chetty, R. (2020). Morphological classification of pancreatic ductal adenocarcinoma that predicts molecular subtypes and correlates with clinical outcome. *Gut*, *69*(2), 317-328. doi:10.1136/gutjnl-2019-318217
- Schmitt, C., Saur, D., Bärthel, S., & Falcomatà, C. (2022). Syngeneic Mouse Orthotopic Allografts to Model Pancreatic Cancer. *J Vis Exp*(188). doi:10.3791/64253

- Schneider, G., Schmidt-Supprian, M., Rad, R., & Saur, D. (2017). Tissue-specific tumorigenesis: context matters. *Nat Rev Cancer*, *17*(4), 239-253. doi:10.1038/nrc.2017.5
- Schönhuber, N., Seidler, B., Schuck, K., Veltkamp, C., Schachtler, C., Zukowska, M., . . . Saur, D. (2014). A next-generation dual-recombinase system for time- and host-specific targeting of pancreatic cancer. *Nat Med*, *20*(11), 1340-1347. doi:10.1038/nm.3646
- Seifert, L., Werba, G., Tiwari, S., Giao Ly, N. N., Allothman, S., Alqunaibit, D., . . . Miller, G. (2016). The necrosome promotes pancreatic oncogenesis via CXCL1 and Mincle-induced immune suppression. *Nature*, *532*(7598), 245-249. doi:10.1038/nature17403
- Siegel, R. L., Miller, K. D., Wagle, N. S., & Jemal, A. (2023). Cancer statistics, 2023. *CA Cancer J Clin*, *73*(1), 17-48. doi:10.3322/caac.21763
- Solinas, G., Germano, G., Mantovani, A., & Allavena, P. (2009). Tumor-associated macrophages (TAM) as major players of the cancer-related inflammation. *J Leukoc Biol*, *86*(5), 1065-1073. doi:10.1189/jlb.0609385
- Spitzer, M. H., Carmi, Y., Reticker-Flynn, N. E., Kwek, S. S., Madhiredy, D., Martins, M. M., . . . Engleman, E. G. (2017). Systemic Immunity Is Required for Effective Cancer Immunotherapy. *Cell*, *168*(3), 487-502.e415. doi:10.1016/j.cell.2016.12.022
- Steele, N. G., Carpenter, E. S., Kemp, S. B., Sirihorachai, V. R., The, S., Delrosario, L., . . . Pasca di Magliano, M. (2020). Multimodal Mapping of the Tumor and Peripheral Blood Immune Landscape in Human Pancreatic Cancer. *Nat Cancer*, *1*(11), 1097-1112. doi:10.1038/s43018-020-00121-4
- Subramanian, A., Tamayo, P., Mootha, V. K., Mukherjee, S., Ebert, B. L., Gillette, M. A., . . . Mesirov, J. P. (2005). Gene set enrichment analysis: a knowledge-based approach for interpreting genome-wide expression profiles. *Proc Natl Acad Sci U S A*, *102*(43), 15545-15550. doi:10.1073/pnas.0506580102
- Sun, G., Li, Z., Rong, D., Zhang, H., Shi, X., Yang, W., . . . Sun, Y. (2021). Single-cell RNA sequencing in cancer: Applications, advances, and emerging challenges. *Mol Ther Oncolytics*, *21*, 183-206. doi:10.1016/j.omto.2021.04.001
- Swietlik, J. J., Bärthel, S., Falcomatà, C., Fink, D., Sinha, A., Cheng, J., . . . Meissner, F. (2023). Cell-selective proteomics segregates pancreatic cancer subtypes by extracellular proteins in tumors and circulation. *Nat Commun*, *14*(1), 2642. doi:10.1038/s41467-023-38171-8
- Tang, Y., Kesavan, P., Nakada, M. T., & Yan, L. (2004). Tumor-stroma interaction: positive feedback regulation of extracellular matrix metalloproteinase inducer (EMMPRIN) expression and matrix metalloproteinase-dependent generation of soluble EMMPRIN. *Mol Cancer Res*, *2*(2), 73-80.
- Tao, J., Yang, G., Zhou, W., Qiu, J., Chen, G., Luo, W., . . . Zhao, Y. (2021). Targeting hypoxic tumor microenvironment in pancreatic cancer. *J Hematol Oncol*, *14*(1), 14. doi:10.1186/s13045-020-01030-w
- Tape, C. J., Ling, S., Dimitriadi, M., McMahon, K. M., Worboys, J. D., Leong, H. S., . . . Jørgensen, C. (2016). Oncogenic KRAS Regulates Tumor Cell Signaling via Stromal Reciprocation. *Cell*, *165*(4), 910-920. doi:10.1016/j.cell.2016.03.029
- Thorsson, V., Gibbs, D. L., Brown, S. D., Wolf, D., Bortone, D. S., Ou Yang, T. H., . . . Shmulevich, I. (2018). The Immune Landscape of Cancer. *Immunity*, *48*(4), 812-830.e814. doi:10.1016/j.immuni.2018.03.023
- Tirosh, I., Izar, B., Prakadan, S. M., Wadsworth, M. H., 2nd, Treacy, D., Trombetta, J. J., . . . Garraway, L. A. (2016). Dissecting the multicellular ecosystem of metastatic melanoma by single-cell RNA-seq. *Science*, *352*(6282), 189-196. doi:10.1126/science.aad0501
- Tjomsland, V., Niklasson, L., Sandström, P., Borch, K., Druid, H., Bratthäll, C., . . . Spångeus, A. (2011). The desmoplastic stroma plays an essential role in the accumulation and modulation of infiltrated immune cells in pancreatic adenocarcinoma. *Clin Dev Immunol*, *2011*, 212810. doi:10.1155/2011/212810
- Traag, V. A., Waltman, L., & van Eck, N. J. (2019). From Louvain to Leiden: guaranteeing well-connected communities. *Sci Rep*, *9*(1), 5233. doi:10.1038/s41598-019-41695-z

- Tsujikawa, T., Kumar, S., Borkar, R. N., Azimi, V., Thibault, G., Chang, Y. H., . . . Coussens, L. M. (2017). Quantitative Multiplex Immunohistochemistry Reveals Myeloid-Inflamed Tumor-Immune Complexity Associated with Poor Prognosis. *Cell Rep*, *19*(1), 203-217. doi:10.1016/j.celrep.2017.03.037
- Tu, M., Klein, L., Espinet, E., Georgomanolis, T., Wegwitz, F., Li, X., . . . Singh, S. K. (2021). TNF- α -producing macrophages determine subtype identity and prognosis via AP1 enhancer reprogramming in pancreatic cancer. *Nat Cancer*, *2*(11), 1185-1203. doi:10.1038/s43018-021-00258-w
- Veglia, F., Sanseviero, E., & Gabrilovich, D. I. (2021). Myeloid-derived suppressor cells in the era of increasing myeloid cell diversity. *Nat Rev Immunol*, *21*(8), 485-498. doi:10.1038/s41577-020-00490-y
- Wang, Y. T., Gou, Y. W., Jin, W. W., Xiao, M., & Fang, H. Y. (2016). Association between alcohol intake and the risk of pancreatic cancer: a dose-response meta-analysis of cohort studies. *BMC Cancer*, *16*, 212. doi:10.1186/s12885-016-2241-1
- Wei, J., Chen, Z., Hu, M., He, Z., Jiang, D., Long, J., & Du, H. (2021). Characterizing Intercellular Communication of Pan-Cancer Reveals SPP1+ Tumor-Associated Macrophage Expanded in Hypoxia and Promoting Cancer Malignancy Through Single-Cell RNA-Seq Data. *Front Cell Dev Biol*, *9*, 749210. doi:10.3389/fcell.2021.749210
- Wellenstein, M. D., & de Visser, K. E. (2018). Cancer-Cell-Intrinsic Mechanisms Shaping the Tumor Immune Landscape. *Immunity*, *48*(3), 399-416. doi:10.1016/j.immuni.2018.03.004
- Whatcott, C. J., Diep, C. H., Jiang, P., Watanabe, A., LoBello, J., Sima, C., . . . Han, H. (2015). Desmoplasia in Primary Tumors and Metastatic Lesions of Pancreatic Cancer. *Clin Cancer Res*, *21*(15), 3561-3568. doi:10.1158/1078-0432.Ccr-14-1051
- Wolf, F. A., Angerer, P., & Theis, F. J. (2018). SCANPY: large-scale single-cell gene expression data analysis. *Genome Biol*, *19*(1), 15. doi:10.1186/s13059-017-1382-0
- Xue, Q., Yan, Y., Zhang, R., & Xiong, H. (2018). Regulation of iNOS on Immune Cells and Its Role in Diseases. *Int J Mol Sci*, *19*(12). doi:10.3390/ijms19123805
- Yang, S., Liu, Q., & Liao, Q. (2020). Tumor-Associated Macrophages in Pancreatic Ductal Adenocarcinoma: Origin, Polarization, Function, and Reprogramming. *Front Cell Dev Biol*, *8*, 607209. doi:10.3389/fcell.2020.607209
- Yu, M., Guan, R., Hong, W., Zhou, Y., Lin, Y., Jin, H., . . . Jian, Z. (2019). Prognostic value of tumor-associated macrophages in pancreatic cancer: a meta-analysis. *Cancer Manag Res*, *11*, 4041-4058. doi:10.2147/cmar.S196951
- Zhang, L., Li, Z., Skrzypczynska, K. M., Fang, Q., Zhang, W., O'Brien, S. A., . . . Yu, X. (2020). Single-Cell Analyses Inform Mechanisms of Myeloid-Targeted Therapies in Colon Cancer. *Cell*, *181*(2), 442-459.e429. doi:10.1016/j.cell.2020.03.048
- Zhang, L., Sanagapalli, S., & Stoita, A. (2018). Challenges in diagnosis of pancreatic cancer. *World J Gastroenterol*, *24*(19), 2047-2060. doi:10.3748/wjg.v24.i19.2047
- Zhang, R., Liu, Q., Peng, J., Wang, M., Gao, X., Liao, Q., & Zhao, Y. (2019). Pancreatic cancer-educated macrophages protect cancer cells from complement-dependent cytotoxicity by up-regulation of CD59. *Cell Death Dis*, *10*(11), 836. doi:10.1038/s41419-019-2065-4
- Zhao, E., Stone, M. R., Ren, X., Guenthoer, J., Smythe, K. S., Pulliam, T., . . . Gottardo, R. (2021). Spatial transcriptomics at subspot resolution with BayesSpace. *Nat Biotechnol*, *39*(11), 1375-1384. doi:10.1038/s41587-021-00935-2
- Zhao, F., Obermann, S., von Wasielewski, R., Haile, L., Manns, M. P., Korangy, F., & Greten, T. F. (2009). Increase in frequency of myeloid-derived suppressor cells in mice with spontaneous pancreatic carcinoma. *Immunology*, *128*(1), 141-149. doi:10.1111/j.1365-2567.2009.03105.x
- Zhu, Y., Herndon, J. M., Sojka, D. K., Kim, K. W., Knolhoff, B. L., Zuo, C., . . . DeNardo, D. G. (2017). Tissue-Resident Macrophages in Pancreatic Ductal Adenocarcinoma Originate from Embryonic Hematopoiesis and Promote Tumor Progression. *Immunity*, *47*(2), 323-338.e326. doi:10.1016/j.immuni.2017.07.014
- Zhu, Y., Knolhoff, B. L., Meyer, M. A., Nywening, T. M., West, B. L., Luo, J., . . . DeNardo, D. G. (2014). CSF1/CSF1R blockade reprograms tumor-infiltrating macrophages and improves response to

T-cell checkpoint immunotherapy in pancreatic cancer models. *Cancer Res*, 74(18), 5057-5069. doi:10.1158/0008-5472.Can-13-3723

Zilionis, R., Engblom, C., Pfirschke, C., Savova, V., Zemmour, D., Saaticioglu, H. D., . . . Klein, A. M. (2019). Single-Cell Transcriptomics of Human and Mouse Lung Cancers Reveals Conserved Myeloid Populations across Individuals and Species. *Immunity*, 50(5), 1317-1334.e1310. doi:10.1016/j.immuni.2019.03.009

7. PUBLICATION

Peer-reviewed article

Selective multi-kinase inhibition sensitizes mesenchymal pancreatic cancer to immune checkpoint blockade by remodeling the tumor microenvironment. Falcomatà, C.*, Baerthel, S.*, Widholz, SA, Schneeweis, C., Montero JJ., Toska, A., Mir, J., Kaltenbacher T, Heetmeyer, J., Swietlik JJ., Cheng J., Teodorescu, B., Reichert O., Schmitt C., **Grabichler, K.**, Coluccio, A., Boniolo, F., Veltkamp, C., Zukowska, M., Vargas, AA., Paik WH., Jesinghaus, M., Steiger, K., Maresch, R., Oellinger, R., Ammon T., Baranov O., Robles MS., Rechenberger, J., Kuster, B., Meissner, F., Reichert, M., Flossdorf, M., Rad, R., Schmidt-Supprian, M., Schneider, G., Saur, D. (2022). *Nature Cancer* (doi:10.1038/s43018-021-00326-1)

8. ACKNOWLEDGEMENTS

At this point I would like to thank everybody who supported me, doing my medical doctor thesis.

First, I would like to thank my supervisor Dieter Saur for giving me the opportunity to work in his group and so getting to know the world of medical research at a deeper view.

I would also like to thank my tutor Marc Schmidt-Supprian for the willingness to support my work.

Special thanks also to Stefanie Bärthel for her great support during the whole research process and also for proofreading my thesis.

In addition, thanks to all colleagues in Saur group for helping me and being available for questions.

Finally, I also like to thank my life partner, my parents and my friends for their invaluable support.